UNIVERSITÀ DEGLI STUDI FIRENZE

DOTTORATO DI RICERCA IN SCIENZE DELLA TERRA

CICLO XXXIII

COORDINATORE Prof. Francalanci Lorella

Climate change and the evolution of human ecology

Dottorando
Dott. Mondanaro Alessandro

(firma)

Tutore
Prof. Rook Lorenzo

UNIVERSITÀ DEGLI STUDI FIRENZE
DST DIPARTIMENTO DI SCIENZE DELLA TERRA

(firma)

Firmato digitalmente da: LORENZO ROOK
Università degli Studi di Firenze
Firmato il: 22-07-2021 08:52:59
Seriale certificato: 663019
Valido dal 30-04-2020 al 30-04-2023

Coordinatore
Prof. Francalanci Lorella

(firma)

UNIVERSITÀ DEGLI STUDI FIRENZE

Firmato digitalmente da: LORELLA FRANCALANCI
Università degli Studi di Firenze
Firmato il: 23-07-2021 00:56:57
Seriale certificato: 662347
Valido dal 29-04-2020 al 29-04-2023

Anni 2017/2020

Table of contents

Abstract

The present thesis focuses on the modifications that our species caused to environment from prehistory to current days investigated through a huge amount of anthropological, faunal, and bioclimatic data. The text is divided in different sections to better describe the relationship between people and the different components of terrestrial ecosystems. Since the *Homo sapiens* history is strictly linked to the evolution of the other human species, I first reviewed how the long-term history of human–environment interaction has affected the evolutionary biology of different human species. Specifically, I investigated the role of the climatic-driven changes in human species distribution assessing the different responses of *Homo* species to climate conditions. In this context, I also tested the role of culture as factor for the widening of human climatic niche.

In the second part of the thesis, I investigated more the relationship between *Homo sapiens* and our phylogenetically and temporally closer human species, that is *Homo neanderthalensis*. I assessed their responses to climatic changes by comparing the temporal evolution of their climatic niche in according to intense climatic oscillations occurred during the Late Pleistocene. I found *Homo sapiens* had greater ecological plasticity over Neanderthals, which probably allowed this species to better react to climatic worsening at 44 and then at 40 ka, a date that almost coincides with estimated Neanderthal's extinction. Moreover, I tested the hypothesis of climatic-driven habitat fragmentation as main cause of Neandethal's demise. As results, data suggest Neanderthals potential habitat appears to be very reduced and fragmented during the last phase of their occupation, whereas for *H. sapiens* did not detect a similar pattern. Lastly, I provided evidences in favor of a social interactions between *H. sapiens* and Neanderthals also supported by genomic evidences rather than the onset of competitive exclusion phenomenon between the two human species.

The last part of the thesis is focused on the role of human influence on Megafauna extinction occurred during the Late Pleistocene. I started analyzing the different trophic role of mammal species within community assembly and ecosystem functioning at large temporal and spatial scales. After that, I focused on the contribution of climatic changes and human appearance on Megafauna's demise in Eurasia. I analyzed how the habitat spatial structure of mammal species changed during the last 200 kylo years. I found a primary role

of climate in Megafauna extinction, whereas I demonstrated human presence was a non-decisive extinction factor for extinct herbivorous megafauna species.

Keywords: *Homo sapiens*, climatic change, Megafauna's extinction, Neanderthal's demise

***Homo sapiens* and other hominin species**

The first section of this thesis focuses on the potential role of climate change in the extinction of human species starting from the first member of *Homo* genus to our species. Unfortunately, although the extinction of human species is one of the most important topics in scientific literature, almost all of the scientific reports dealing with the extinction of past *Homo* species mostly debated about disappearance of a single taxon, *H. neanderthalensis*, and almost all existing works point to either climate change or to the competition with the more technologically advanced *H. sapiens* as the potential causal explanations (Gilpin et al. 2016; Sørensen 2011).

In *("Past extinctions of Homo species coincided with increased vulnerability to climatic change",* Raia et al. 2020*)*, we fill this gap by investigating climatic niche evolution in *Homo*, using a high-resolution paleoclimatic dataset. Specifically, we used the paleoclimatic GCM PLASIM-GENIE emulator developed by Holden and colleagues (Holden et al. 2019) in order to retrieve a high-detailed climatic data relative to: (1) minimum seasonal temperature, (2) maximum seasonal temperature, (3) minimum seasonal precipitation, (4) maximum seasonal precipitation, and (5) net primary productivity. This set of climatic variables temporally covers the last 5 million years with a 1000-year time resolution. As regards, the spatial resolution, the native resolution of climatic data was downscaled to obtain a more-defined gridded resolution of 0.5 degrees. We temporally and geographically combined this large amount of paleoclimatic data with human fossil occurrences gathered during my PhD. We considered only six human species, *H. habilis*, *H. ergaster*, *H. erectus*, *H. heidelbergensis*, *H. neanderthalensis*, and *H. sapiens* because the fossil records of the other human species were too much restricted stratigraphically and geographically to analyze their climatic niche evolution. We repeated the statistical analyses testing different taxonomic species attributions due to the taxonomic uncertainty of some human remains. Consequently, for each of the six species, we identified a ''core'' fossil record, restricted only to reasonably certain attributions of individual fossil specimen and archaeological layers. Then, we repeated the analyses under a less conservative ''extended'' subdivision of the fossil record, whereby individual remains and archaeological layers without a unique taxonomic attribution were attributed to more than one candidate human species. Overall, human fossil record included 2,754 age estimates, over 759 fossil localities.

To account for the effect of dating uncertainty, we produced, for each occurrence, a uniform distribution spanning from the minimum to the maximum of the age estimate. Then, we randomly sampled a single date within this range, and repeated this procedure 100 times in order to obtain different available subset of data. Since we were interested in quantifying differences among *Homo* species in their climatic requirements in a geographically explicit context and analyzing how these requirements change over time, we decided to quantify the degree of overlap of different climatic niches following the approach described in Broennimann et al. 2012. We applied kernel smoothers to densities of species occurrence in gridded environmental space to calculate metrics of niche overlap and test hypotheses regarding niche conservatism (Broennimann et al. 2012). It is possible to apply this framework to calculate the niche overlap among the same species but at different times. In agreement with our aim, for each species and subset of data, we randomly generated a set of 10,000 background points, which were used as pseudoabsences together with observed presences. The 10,000 pseudoabsences were subdivided across the time periods where each species occurred, proportionally to the number of fossil occurrences falling within each time bin. As sampling areas for background points, we utilized the well-known biogeographic boundaries for each species. Specifically, we sampled Africa for *H. habilis* and *H. ergaster*, Eurasia for *H. erectus* and *H. neanderthalensis*, and a combination of both areas for *H. heidelbergensis* and *H. sapiens*. To reduce the risk of sampling non-accessible areas according to species dispersal abilities, we generated background points for each species within a specific area drawn as a 1,000 km buffer around the convex hull surrounding all known species occurrences. Lastly, we geographically and temporally associated the output 100 subset of data, in which presence and background points were collapsed together, with climatic data.

For each of 100 replicates, we divided fossil record into discrete, consecutive time bins, minimizing the variance of the time bin lengths and number of localities, by means of likelihood optimization. This maximum likelihood optimization function was been developed specifically to be used in our article. We repeated this procedure for each *Homo* species and for both “core” and “extended” records. Since the fossil record of *H. neanderthalensis* and *H. sapiens* is vastly richer than that of earlier *Homo* species, we divided their record in 1 kyr time bins without applying the likelihood optimization. Even if poor, the record of each human species

follows a Gaussian distribution, being rare both at the beginning and toward the end of their existence. The same pattern does not occur with *H. neanderthalensis* and *H. sapiens*. In fact, their fossil distribution is highly skewed towards recent time due to the increase of potential preservation of fossil specimens and the accuracy of method dating (i.e., the applicability of C^{14} radiometric method). Only for these two species, we calculated the skewness of the distribution of age estimates and removed the localities in the right (i.e., older age) of the age estimate distribution until skew included the 90% of the total number of occurrences.

We temporally ordered the time bin from the older to more recent for each human species. Then, we used the Schoener' D metric (Schoener 1970) in order to measure the degree of overlap between the climatic niche realized by the species within each temporal bin (bin climatic niche, BCN) and the niche the species realized throughout its entire existence (evolutionary climatic niche, ECN). Taking into account both the climatic conditions where the species occurred and the background climatic variability during the temporal interval covered by the bin, Schoener's D values can span from low (D = 0) to perfect overlap (D = 1). Since the BCN is necessarily included within the ECN, low values of Schoener's D indicate that BCN is small as compared to the ECN, meaning that during the bin duration the species experienced a restricted or peripheral portion of the total climatic variation represented by its ECN. Conversely, at Schoener's D = 1 the species experienced, during the bin, as much climatic variation as throughout its existence.

Our results suggest *Homo* species retain the same climatic preference for most of their existence in according to niche conservatism process. But for three species only, i.e. *H. heidelbergensis*, *H. erectus*, and *H. neanderthalensis*, we found a sudden, statistically significant drop in D just before extinction, indicating that their climatic niche shrunk or reduced just before they vanished (Figure 1).

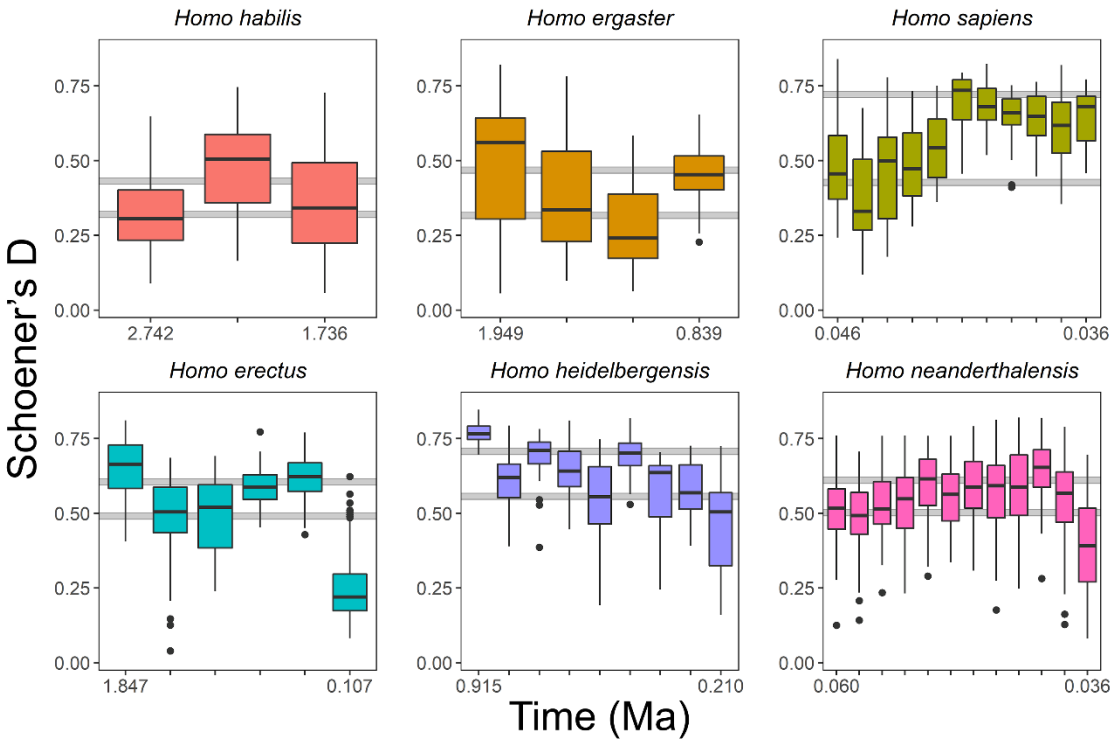

Figure 1. Degree of niche overlap between a niche occupied during a specific time bin (BCN) and the species evolutionary total niche (ECN) (measured in terms of Schoener's D values, y axis), using the core record. Image from Raia et al. 2020.

These patterns remain almost the same whether the ''core'' or ''extended'' fossil records are used.

We determined the BCN position within the ECN volume through time, calculating the multivariate Euclidean distance between the barycenter of the ECN and the barycenter of each BCN. The temporal trend of this distance provides detailed information about the different degree of overlap. Specifically, two BCNs could show the same distance from ECN but have different degrees of overlap due to different size of BCNs area. Similarly, two BCNs overlapping to ECN to the same degree of overlap could lay at different distances meaning that one of the two BCN encloses an unusual or peripheral part of total climatic variation of ECN. The results of this analysis indicate that two extinct species, *H. heidelbergensis* and *H. erectus* experienced highly unusual climatic conditions before their extinction (i.e., during their respective last bins) with relatively restricted climatic range, whereas the realized climatic niche in *H. neanderthalensis* last bin was narrow, but

not unusual for the species. For other human species, we did not detect similar patterns.

To better explore the causes of the significant drops in the last bin occurred in the previous described three extinct species only, we hypothesized a significant relationship between climatic change and their extinction risk. For this purpose, we applied climatic niche factor analysis (CNFA, Rinnan & Lowler 2019). CNFA is used in conservation studies to quantify aspects of sensitivity, exposure and vulnerability to climate change as well, using future projections of global climate conditions. Specifically, we utilized CNFA measure to calculate climate change-driven vulnerability during the last bin of extinct species by using their realized climatic niche during their penultimate bin, while climatic conditions they faced during their last bin are selected as future projections of climate changes. We developed CNFA over the same 100 replicates for each species. We performed vulnerability test on *H. sapiens* to detect potential differences between extinct species and a species without drop in Schoener's D in the last bin. Vulnerability values were then compared among species by means of ANOVA and post-hoc Tukey HSD tests. Results of CNFA analysis demonstrated clear differences in vulnerability between *H. sapiens* and the significantly more vulnerable extinct species (Figure 2).

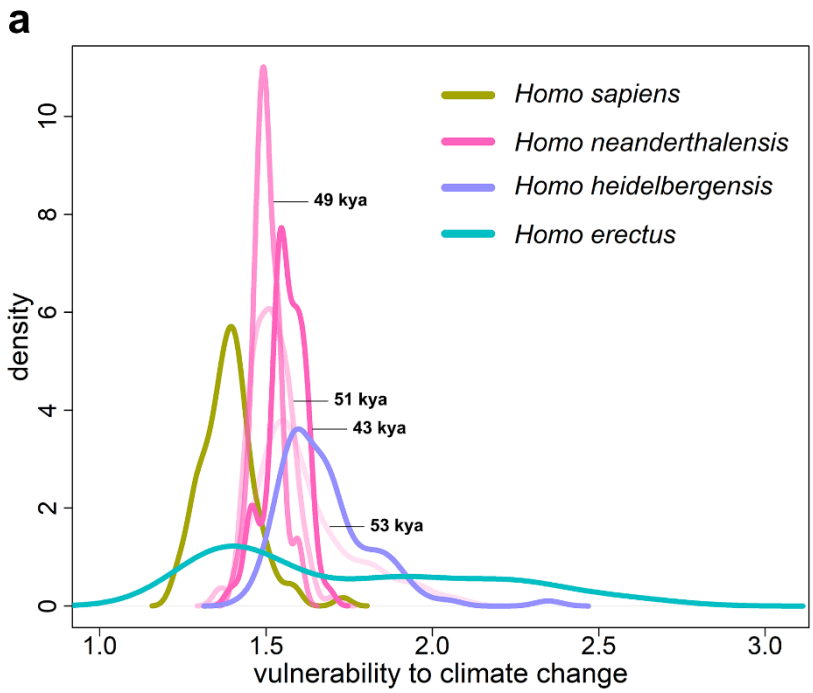

Figure 2. Density plots of climate-induced vulnerability to extinction as predicted by CNFA analysis. Image from Raia et al. 2020

All this confirmed climate change was fully involved in the extinction in past *Homo* species, which were not able to counter rapid climatic changes. As proof of this, the extinct species became restricted to unfavorable or otherwise narrowly shaped climatic conditions just before their extinction. In contrast, for the early species of genus *Homo* (i.e. *Homo habilis* and *Homo ergaster*), the absence of the drop in D in the last bin could be artificial, as the grouping might include a species that went extinct plus its anagenetic descendant. For instance, we did not observe any significant pattern in Schoener' D over time for *H. ergaster* because it more likely represents a mere regional variant ("paleodeme" *sensu* Rightime et al. 2006) of more geographically and temporally extended *H. erectus* (Rightmire et al. 2009). On the other hand, we demonstrated vulnerability to climate changes of *H. sapiens* appear lower compared to the extinct species. Consequently, we can assume that this higher climatic tolerance allowed it to survive to all the changes in climate it experienced during its existence.

In the second work related to this section, we investigated about how the acquisition of advanced cultural abilities could have affected the geographical dispersal of past *Homo* species. Specifically, we hypothesized that technological innovations allowed past *Homo* species to experience a wide spectrum of climatic conditions.

In "*A major change in rate of climate niche envelope evolution during hominid history*", Mondanaro et al. 2020), we investigated the role of culture in the evolution of climatic niche during the human history. We tested the idea that only *H. sapiens* was able to take advantage from its cultural innovations to inhabit almost all terrestrial ecosystems. This idea is supported by evidences of new advanced prehistoric cultures developed from 40 000 years ago in Europe, that almost coincides with Upper Paleolithic period. Many works demonstrated the transition from the Middle to Upper Paleolithic represents a major turning point in human evolution from the cultural, demographic, and geographical expansions point of views (Greenbaum et al. 2019). Unsurprisingly, many authors refer to this period as "Upper Paleolithic Revolution" (UPR) designating a profound change from the previous Middle Paleolithic tool manufacture techniques to those of blade-

dominated artifact assemblages, with the proliferation of particular tool types such as end-scrapers and burins, as well as bone and antler objects, along with mobile art items and cave paintings (Bar-Yosef 2007). Intriguing question were raised concerning the origins and the chronological framework of UPR. Anthropologists proposed two main theories about this debated point: the transition to the Upper Paleolithic was a sudden global event brought in Eurasia by first Anatomically Modern Humans (AMH) populations. In accord with this theory, the UPR was the hallmarks of *Homo sapiens* culture, who was able to take advantages from its advanced cognitive abilities to make the so called "great cultural leap forward" (Diamond 1989; Bar-Yosef 2002). On the other hand, other researchers support a more gradual cultural transition in which *H. sapiens* was not the unique bearer of the cultural advances associated to UPR (Van Peer 2004; Greenbaum et al. 2019). The latter hypothesis was corroborated by new discoveries which increased the knowledges about the Neanderthal's culture. In Bruniquel Cave, in France, Neanderthal group was able to elaborate constructions made with hundreds of partially calibrated, broken stalagmites that appear to have been deliberately moved and placed in specific locations, along with the presence of several intentionally heated zones. This suggest Neanderthal possessed a high complex level of spatial organization (Jaubert et al. 2016). Similarly, the discovery of the first musical instruments associated to Neanderthal's occupation in Divje Babe I, in Slovenia, traces back the first evidence of cultural modernity before the arrival of *H. sapiens* in Europe (Turk et al. 2018). Additional evidences of birch bark tar, art, and shell beads demonstrated that Neanderthals were not cognitively inferior to modern humans (Hardy et al. 2020).

As regards the geographical expansion, *H*. sapien*s* is considered the only species in the *Homo* genus able to colonize cold climate regions through a genuinely cultural process, driven by its technology, including the mastering of fire, ever improving clothing craftsmanship, and construction of shelters. This is particularly relevant to human evolution since it is been demonstrated extensive environmental modification through cultural practices have influenced our evolutionary history (Wollstonecroft 2011), in keeping with an ecological theory known as "cultural niche construction" (Laland et al. 2001). According with this perspective, niche construction is recognized as an evolutionary process where ecological inheritance plays a parallel role to genetic inheritance (Laland & O'brien, 2011). As reported by Lewontin in 1983, "'*Organisms do not adapt*

to their environments; they construct them out of the bits and pieces of the external world"'. Since culturally transmitted response is strictly linked to genetic response, researchers argued about human species were fully involved in this cultural process. Indeed, culturally transmitted response could fail, perhaps because the population lacks the necessary knowledge or technology (Laland et al. 2007). For some authors, the process of cultural niche construction through which human cultural traits have changed the human adaptive niche and in turn selective pressures and ecological inheritance, traces back to the very emergence of the genus *Homo* at some 2.5 million years ago (Antón & Snodgrass, 2012; Antón et al. 2014). Stone artifact production and social interactions may have allowed the past *Homo* species not only to escape their biological constraints but also to actively change the environmental and ecological niches of other species (Hiscock, 2014, Fuentes et al. 2010). Moreover, even in the case of harsh climatic regimes beyond human tolerance, human 'cultural niche construction' would have strongly affected the intensity of selection, for instance, by manufacturing clothes or shelters, or controlling fire (Laland et al. 2007). Unfortunately, clothing manufacturing leaves very little in the way of fossil remains whereas evidence of use of fire are very rare and occasional in the anthropological record (Gowlett 2016). Consequently, clear traces of cultural modernity are attested only for the last 50 kilo years. This could give some support to a sudden leap forward during the Upper Paleolithic Revolution restricted to our species only. In contrast, human fossil record suggests other *Homo* species were able to expand their geographical distribution to Northern Europe and Western Siberia, despite the contemporaneous establishment of full glacial cycles made the climate regime a real challenge for human survival. Archaeological findings in Happisburgh and Pakefield (UK) date the earliest occurrence of *Homo* at the southern edge of the boreal zone at some 0.7–0.9 Ma (Parfitt et al. 2010).

In Mondanaro et al. 2020, we estimated the period when the limits of human climatic tolerance expand, as well as which species were involved. We did not specifically address the cultural and social adaptations that might underlie such tolerance but rather consider the implications of our findings for the timing of such adaptations. We modelled the evolution of climatic tolerance (i.e. niche) limits in the *Homo* genus by associating paleoclimatic values retrieved from Holden et al. 2019, with Hominin's fossil occurrences. As done in the previous paper of this thesis, we excluded the hominin species with a stratigraphically and

geographically record too restricted to analyze their climatic niche evolution. After this step, human fossil data set included 2,597 occurrences of hominin remains and artifacts associated with 727 archaeological sites. The time range of our record spanned from the first occurrence of Australopiths in East Africa dated to some 4.2 Ma to the definitive advent of *H. sapiens* in Eurasia almost coincident with the demise of *H. neanderthalensis* dated at 0.040 Ma (Higham et al. 2020).

We aimed testing the hypothesis that *H. sapiens* developed greater climatic tolerance relative to *H. heidelbergensis* and *H. neanderthalensis* against the alternative that the exploration of climates outside natural physiological limits had already begun before the appearance of our species in according to a more gradual process of niche construction. For this purpose, we accounted for the effect of dating uncertainty randomly sampled a single date within the uniform distribution of possible dates related to each age estimate and repeated this procedure 100 times in order to obtain different subsets of data (see above). After that, we used the same bioclimatic variables described in Raia et al. 2020 and combined them to anthropological data, following the same procedure described in Raia et al. 2020. For each replicate, we aimed to estimate the rate of change of climatic tolerance limits across the human phylogenetic tree and searched for possible shifts in the rate. First, we apply the phylogenetic ridge regression, a phylogenetic comparative method developed by our research group ("RRphylo"; Castiglione et al. 2018), to analyze the temporal dynamic of the climatic niche evolution in the hominin species. RRphylo allows to compute evolutionary rates for each branch of the phylogeny and to estimate the ancestral phenotypes at each node of the tree (Raia et al. 2018; Melchionna et al. 2020a). We pruned the primate phylogeny used in Melchionna et al. 2020 to obtain a human phylogeny composed by 10 hominin species.

In our case, climatic tolerance limits for each hominin species (i.e. temperature, precipitation and NPP minima and maxima) represented the phenotypes at the tips of the tree while a positive/negative shift in the rate of evolution indicated an enlargement/contraction of human climatic tolerance. A positive shift could coincide with the acquisition of the capacity to develop cold climate-related technological skills and cultural adaptations at the time of the shift. Conversely, if either no rate shift occurred, the colonization of Northern habitats would not be indicative of any sudden increase in the ability to face environmental harshness.

Furthermore, we accounted for the phylogenetic uncertainty by changing the tree node ages and the tree topology. This procedure allowed us to pair combined each replicate to as many different hominin phylogeny in order to obtain the input data for RRphylo function. By incorporating both dating and phylogenetic uncertainty in this way, we were able to define an overall "habitat quality" (HQ) metric, representing the number of times (out of 100 replicates) a geographic cell of landscape layer (i.e. Old World in our case) was found habitable (i.e. fell within climatic tolerance limits estimated at the tree node by RRphylo) for a given human ancestor in the tree.

Since these values are estimated, rather than observed, to assess the association between the location of fossil localities and habitat quality, we selected the fossil occurrences of its descendants for each ancestral species estimates. To measure this association, we calculated the Area Under receiver operator Curve (AUC) averaging over the 100 replicates. AUC theoretically ranges from 0 to 1 indicating a negative and positive relationship between variables, respectively. To obtain a null distribution of AUC values and assess significance for the AUC, for each node in the tree we sampled 100 times as many point occurrences as with the real data (i.e. the sum of fossil occurrences of the species descending from that node) within the biogeographic domain of the species groups (i.e. the descendants to a given node in the tree). We found that despite the enormous geographic variation in both the preservation potential and the intensity of paleontological sampling, there is a strong association between the geographic position of archaeological remains and the inferred suitability of the environmental conditions for all nodes in the hominin tree. This result suggests that climatic variation in time and space strongly controlled the geographic ranges of our ancestors.

To test whether individual clades evolved at significantly different rates as compared to the rest of the tree, we used the function "*search.shift*" included in RRphylo R package. We detected an evolutionary rates shift coincident with common ancestor of *H.sapiens*, *H. neanderthalensis*, and *H. heidelbergensis* (Modern *Homo* species; MHS) (Figure 3).

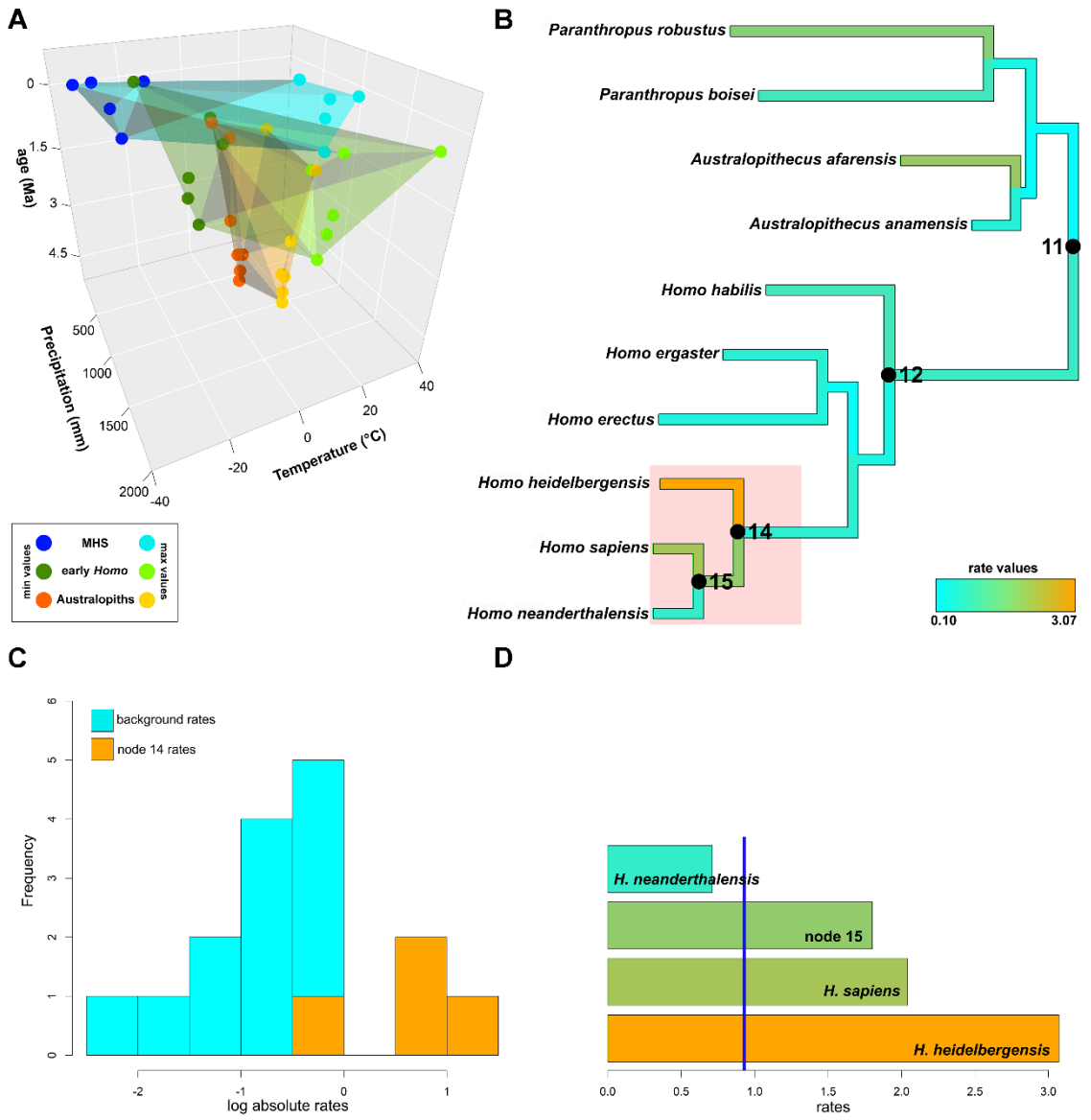

Figure 3. Climatic niche evolution in Hominins: (A) Three-dimensional plot of the climatic niche space occupied by the hominin clades through time. (B) The hominin tree used in this study. The branch colors are proportional to the multivariate rate of climatic niche evolution for each branch in the tree. At the MHS common ancestor (14), an acceleration in the rate of evolution in climatic tolerance limits occurs (shaded area); (C) The distribution of the rates of niche evolution for the MHS clade (orange) compared to the rest of the branches in the tree (light blue); (D) The individual rates of niche evolution for the tree branches forming the MHS clade. The average rate for the entire tree is indicated by the vertical blue line. MHS = modern *Homo* species, EHS = *Homo* species exclusive of MHS, Australopiths = species in the genus

***Paranthropus* and *Australopithecus*. Image from Mondanaro et al. 2020.**

To look for possible evolutionary trends in climatic tolerances over time, we used another function included in RRphylo package, called "*search.trend*" (Castiglione et al. 2019). In search.trend, evolutionary rates and phenotypes (including the phenotypic estimates at the nodes) are regressed against their age and the resulting slopes compared to slopes randomly generated under the Brownian motion model of evolution, which is a model assuming no temporal trend is present in the data. As a result, we found significant trends in both minimum temperature and precipitation along human phylogeny occurred 97 times (97 out 100 replicates), whereas no trend was found in the maximum temperatures, maximum precipitation and NPP (Figure 4).

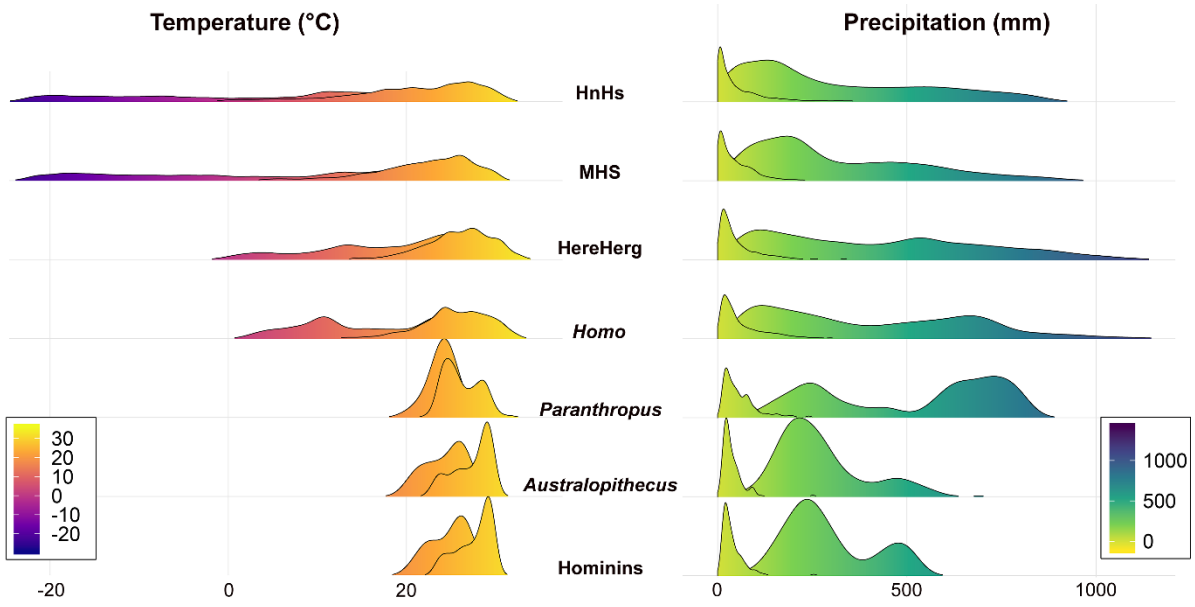

Figure 4. Estimated temperature and precipitation ranges at several nodes in the human phylogenetic tree. The individual rows represent the density distribution of minimum and maximum temperature and precipitation, respectively, collapsed together. HnHs = common ancestor to *H. neanderthalensis* and *H. sapiens*, MHS = common ancestor to *H. heidelbergensis*, *H. neanderthalensis*, and *H. sapiens* HereHerg = common ancestor to *H. erectus* and *H. ergaster*, *Homo* = common ancestor

to *Homo* species, *Paranthropus* = common ancestor to all *Paranthropus* species, *Australopithecus* = common ancestor to all *Australopithecus* species, Hominins = common ancestor to hominins.

The detected positive shift coincident with the ancestors of MHS (Figure 3) was not an exclusively biological process. Although the common ancestor to MHS was an African species probably adapted to savanna-like habitat (Profico et al. 2016), the estimated values agree qualitatively with the notion that a sudden widening of climatic niche limits occurred with the advent of this ancestor. We recorded a massive increase in the estimated range of thermal conditions suitable for the MHS clade (marked by a 20°C decrease in minimum temperature of the coldest season as compared to the hominin closer to tree root). Indeed, we found that in African species and ancestors, the average temperature of the coldest quarter of the year was no less than 9.4°C, meaning that the winter chill is unlikely to have been a problem for them. In contrast, within the range of temperatures experienced by *H. heidelbergensis*, the coldest quarter of the year was as cold as −12.3°C, suggesting specific technological and cultural adaptations were needed to counter the risk of hypothermia and to live in the highly seasonal, cold northern environments (Ulijaszek & Strickland 1993; Ellison et al. 2005; Gilligan 2007). Among the wide spectrum of possible cultural adaptations, we can mention the use of clothing (Amanzougaghene et al., 2019), thrown spears (Lenoir & Villa, 2006) or adhesives (Cârciumaru et al., 2012), and enhanced healthcare practices (Spikins et al., 2019), whereas there are only occasional or indirect evidences of fire use during the Middle Pleistocene (Gowlett 2016; Organ et al. 2011). A very recent article revealed the emergence of brain asymmetry and expansion of cortical areas processes usually linked with advanced cognitive skills back to *H. heidelbergensis* (Melchionna et al. 2020b). Consequently, these findings support the connection between cognitive abilities, human cultural traits and geographic expansion as proposed by cultural niche construction theory.

Overall, our results demonstrated that behavioral modernity, interpreted as the ability to use technology and culture innovations to overcome the constraints imposed by environment on the geographic distribution, is not restricted to *H. sapiens* and to Upper Paleolithic period.

***Homo sapiens* and Neanderthals**

The first paper of this section is ("*Fragmentation of Neanderthals' pre-extinction distribution by climate change*"; Melchionna et al., 2018). It perfectly falls in the huge discussion about the cause of Neanderthal's demise. Higham and colleagues used an enormous collection of dating associated with last Neanderthal's sites and a very advanced method technique to construct robust chronology of Neanderthal disappearance. The chronological Bayesian model built by these authors estimated the extinction of Neanderthals some 40 ka (Higham et al. 2014) during marine isotopic stage 3 (MIS 3), and almost in coincidence with Heinrich Event 4, which is a sudden, global shift towards colder temperatures (HE4, Van Meerbeeck et al. 2009). However, these findings did not fully solve the issue concerning the causes of Neanderthal's extinction. Overall, most of the authors attributed the extinction of Neanderthals to either climatic change (Raia et al. 2020; Sepulchre et al. 2007), or to the effect of competition with AMHs (Hortolà & Martínez-Navarro 2013; Banks et al. 2008). To shed light on this topic, we used Species Distribution Modelling (SDMs) to quantify and compare statistically the inferred climatic niches of *H. sapiens* and *H. neanderthalensis* in Western Eurasia during the last 8 ka of Neanderthals existence.

We studied climatic niche evolution and overlap in the two *Homo* species identifying their optimal climatic conditions and the degree of fragmentation of both climatic niches over time.

We collected a total of 135 fossil occurrences for *H. neanderthalensis* and 104 occurrences for *H. sapiens* spanning from 60 to 36 ka. At the same time, we downloaded the climatic data coming from the paleoclimate model generated by Singarayer and Valdes (2010). This model is provided with a temporal resolution of 4 kyr and a 0.5° of spatial resolution after a downscaling step performed by Maiorano et al. 2013. Specifically, the following four climatic predictors were derived: i) mean temperature during summer, ii) mean temperature during winter, iii) mean precipitation during summer and iv) mean precipitation during winter.

To model species distributions we pooled human fossil occurrences and climatic data together across all the time intervals chosen for the analysis. To minimize the problem of dating accuracy, we used the same preliminary procedure described above (Raia et al. 2020; Mondanaro et al. 2020) in order to obtain 100 subsets of data available for SDM calibration.

For each species and SDM replicate, we randomly generated a set of 10,000 background points over Eurasia, which were used as pseudo-absences together with observed presences. The 10,000 pseudo-absences were subdivided across the time periods where each species occurred, proportionally to the size of the occurrence records falling into each interval. SDMs were calibrated using an ensemble forecasting approach, as implemented in the biomod2 R-package (Thuiller et al. 2009). We tested the following four modelling algorithms: Generalized Linear Models (GLMs); Generalized Additive Models (GAMs), Generalized Boosted Regression Models (GBMs) and Maximum Entropy (MAXENT). We used a bootstrap validation design in which each species occurrence dataset was randomly split into a 70% sample, used for the calibration of the model, and the remaining 30%, used to evaluate the model performance. Models' predictive performance was assessed measuring the area under the receiver operating characteristic curve (AUC), and Boyce index (Hirzel et al. 2006). The splitting procedure for model evaluation was repeated 10 times and evaluation scores and projections were averaged. To avoid using poorly calibrated models, the projections from the models with AUC < 0.7 were discarded in the subsequent analyses. Models were averaged calculating a weighted mean by model's AUC (Marmion et al. 2009). SDMs were projected over Eurasia on three specific moments, i.e. at 48 ka, at 44 ka, and at 40 ka, in keeping with the temporal resolution of the climatic data. The three model projections were transformed into binary maps of species presence and absence, using the threshold that maximizes the sum of sensitivity and specificity (Di Febbraro et al. 2015; Maiorano et al. 2013).

To quantify the degree of fragmentation of climatic niches, we calculated a set of landscape metrics developed in Fragstats R-software (McGarigal et al. 2012). Specifically, these metrics analyze the degree of structural connectivity between optimal habitat patches as predicted by SDMs for the two human species separately and at each time projection. We chose the following metrics: Number of Patches (NP), Area_weighted mean patch area (AREA_AM), Area_weighted mean patch Euclidean distance (ENN_AM), Clumpiness Index (CLUMPY); Proportion of Like Adjacencies (PLADJ); Patch Cohesion Index (COHESION); Effective Mesh Size (MESH); Splitting Index (SPLIT) and Aggregation Index (AI).

Optimal habitat patches for each species at the three selected intervals were identified by progressively binarizing continuous SDMs predictions (i.e. averaged from the 100 replicates) according to a threshold

ranging from the 50th to the 95th percentile of the suitability values predicted by the ensemble forecasting, with a step of 1. The landscape metrics were then calculated for each of the 46 (50th to 95th percentile) resulting binary maps. Such metrics are highly dependent on the amount of suitable habitat for a species in a landscape and tend to be strongly correlated to each other (Wang et al., 2014). Therefore, it is often difficult to disentangle the distinct components of landscape structure (e.g., the amount and configuration of habitat) when analyzing landscape patterns (Wang et al., 2014). To minimize this issue, we excluded those landscape metrics exhibiting a high mutual correlation, i.e. Pearson $|r| > 0.7$, with the area of the predicted distribution for each species and time interval. Subsequently, we excluded highly correlated landscape metrics by considering the same correlation threshold. The remaining metrics, that are NP, ENN_AM and COHESION, along with their interaction terms with time intervals, were included into a GLM with a binomial response (*H. neanderthalensis* ["0"] vs *H. sapiens* ["1"]), in order to test for statistically significant differences in these metrics among the optimal habitat patches of the two species. We selected the best-fit model by using Akaike Information Criterion (AIC) and computed Nagelkerke's adjusted R^2 to assess GLM goodness-of-fit. Moreover, we derived the climatic preferences of two *Homo* species by using the Ecological Niche Factor Analysis (ENFA, Hirzel et al., 2002). ENFA analyzes the position of the niche in the ecological space by comparing the distribution of ecological predictors values between species occurrences and the landscape area. Such niche position is evaluated by calculating the *marginality* i.e. the squared distance of the niche barycenter from the mean available habitat, and *tolerance* i.e. the reciprocal of specialization (Hirzel et al., 2002). A high marginality indicates that a species occurs in very peripheral environments as compared to the background environmental variation. High specialization corresponds to a restricted niche relative to the habitat conditions available to the species (Hirzel et al., 2002). High tolerance indicates that a species tolerates large climatic variations from its optimum conditions (Simard et al., 2009) and therefore shows a potential higher niche breadth compared to species with low tolerance for uncommon climatic condition (Braunisch et al., 2008). We calculated marginality and tolerance for the two *Homo* species at each time interval and for each of the 100 dating replicated datasets. Statistical differences in niche marginality and specialization through time points between *H. neanderthalensis* and *H. sapiens* were evaluated using ANOVA

and post hoc Tukey Honest Significant Differences test (Tukey's HSD test).

In a similar way to Raia et al. 2020, we estimated the degree of niche overlap between human species. But this time, we evaluated the overlap between two species rather than using the climatic niches of the same species but realized in different time bins. To this aim, we calculated the niches in a gridded and smoothed Principal Component Analysis (PCA) environmental space, taking into account climatic variables over the study area for each time frame, as described in Broennimann et al. (2012). We represented the available climatic space of the two species (i.e. all the climatic conditions occurring in Eurasia during the selected time period) by pooling climatic data together for the 60–36 ka time intervals (climatic data occur in 4 kyr long frames) and by using these to calibrate a PCA. Subsequently, we projected the values of climate variables corresponding to species locations in the 48 ka, 44 ka and 40 ka time steps into the PCA space to delineate the partial niches of the two *Homo* species in these three different moments. The degree of niche overlap was eventually estimated by means of Schoener's D (Schoener 1970; Raia et al. 2020) ranging from 0 (no overlap) to 1 (complete overlap).

By using SDMs model output, we obtained the response curves of both species to each climatic variable. We found both *Homo* species distributions as primarily driven by temperature during the coldest and the warmest seasons. Response curves of both species are highly overlapping, suggesting close similarity between Neanderthals' and AMH's optimum climatic preferences. However, *H. sapiens* curve tails exceeded those of *H. neanderthalensis* for three of four predictors, namely temperature during summer and both precipitation variables, suggesting a wider tolerance to these predictors by *H. sapiens* (Figure 5).

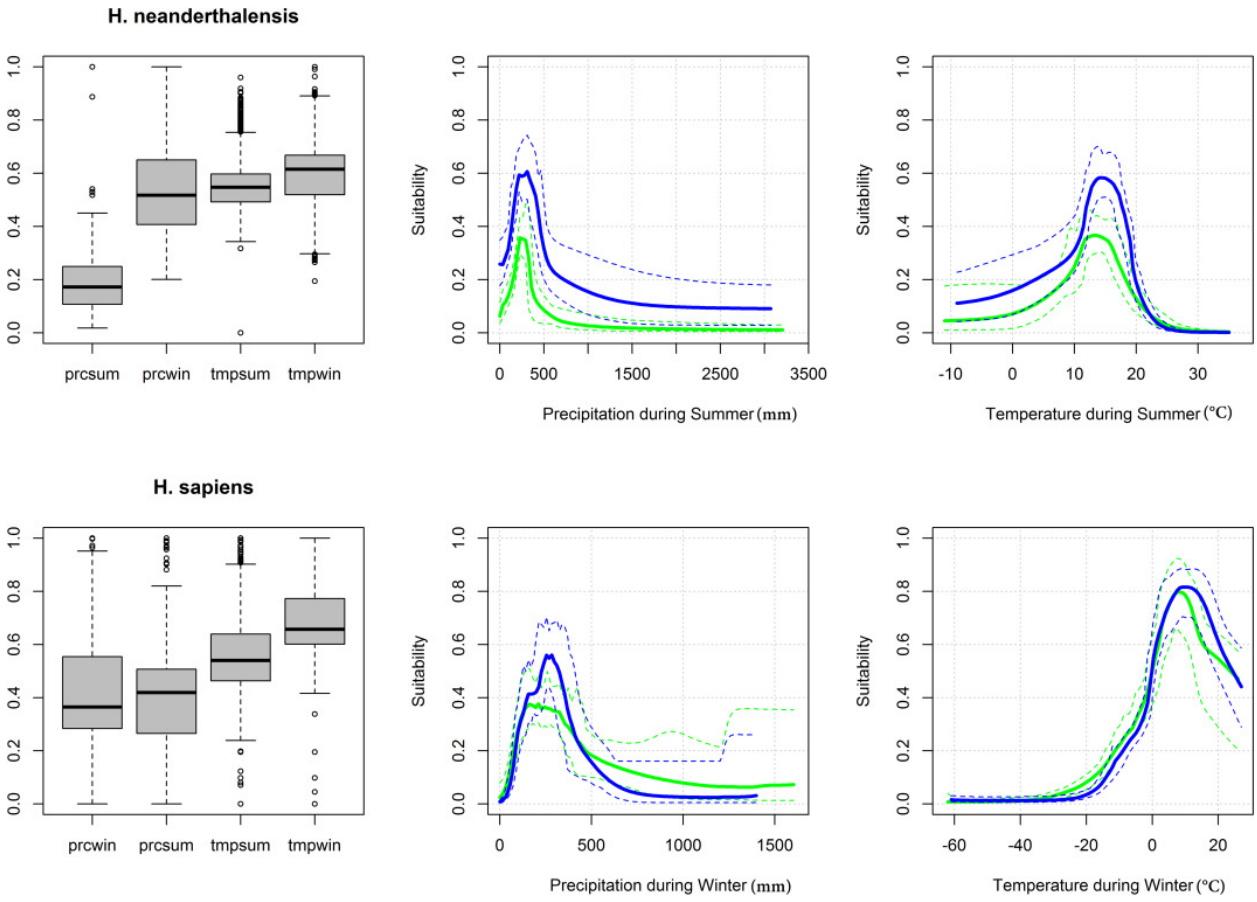

Figure 5. Relative contribution to the models and related response curves of each climate predictor. Variables in the box plots are listed in order of importance from left (low importance) to right (high importance). Response curves depict the variation of the probability of presence versus each climatic variable, with blue (green) curves referring to *H. neanderthalensis* (*H. sapiens*). Dotted lines represent the range interval over the 100 SDMs run per species in order to account for dating uncertainty. Image from Melchionna et al. 2018.

Landscape analyses show a high reduction of predicted distribution over time in term of geographical range size for both *Homo* species. However, the potential geographic range of *H. sapiens* was constantly larger than the Neanderthal's range.

The resulting GLM outcomes found a significantly higher number of patches in *H. neanderthalensis* compared to *H. sapiens*, irrespectively of the time steps, while there was no significant difference in mean patch distance between the two *Homo* species distributions. In addition, a statistically significant association

emerged between the distributions of *H. neanderthalensis* and lower COHESION values. Overall, these results demonstrated the number of isolated patches within the Neanderthal range is statistically higher than with *H. sapiens*, and these patches are less connected to each other. Importantly, we detected a clear temporal trend in optimal patches (i.e. above 95th percentile of the suitability values). Specifically, optimal patches predicted at 48 ka shown a negligible difference in their spatial configuration between the two human species, but structural connectivity within *H. sapiens* range remained almost constant over time, whereas that of Neanderthals steadily deteriorated (Figure 6).

ANOVA performed on ENFA outcome values indicated significant differences in both niche marginality ($F = 5$, $df = 151.3$, $p < 0.001$) and tolerance ($F = 5$, $df = 579.9$, $p < 0.001$) between the two *Homo* species and the three time moments. The related post hoc Tukey HSD test reported significantly higher niche marginality by *H. neanderthalensis* irrespectively of the time interval. On the other hand, *H. sapiens* significantly increased its niche tolerance through time.

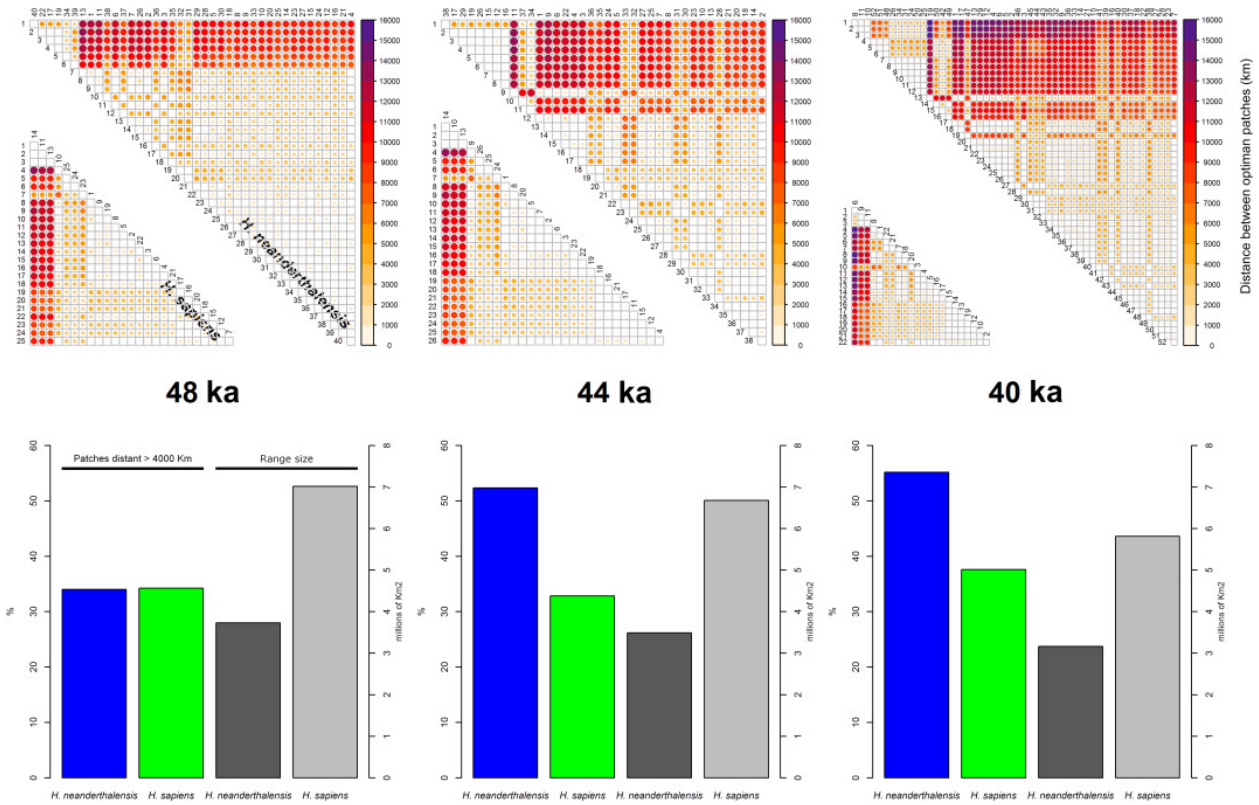

Figure 6. Evolution of optimal habitats in Neanderthals and *H. sapiens*. Dots depict the linear distance in kilometers between optimal patches pairs (i.e. above the 95th percentile of the suitability values predicted

by the ensemble forecasting). Distance increases from white to purple and is proportional to dots size. Row and column numbers refer to the individual patch ID. Blue (green) columns in bar plots summarize the percentage of optimal patches pairs >4000 km apart for *H. neanderthalensis* (*H. sapiens*) in the three time points. Dark grey (light grey) bars indicate range size of *H. neanderthalensis* (*H. sapiens*) in millions square kilometers. Image from Melchionna et al. 2018.

As for niche overlap tests, the first two PCA axes accounted for 76% of the total variance in the data (~52% for PC1 and ~24% for PC2). In all time frames, the niches of two human species shown high overlap (Schoener's D values >0.6) with a maximum overlap degree at 44 ka (i.e. Schoener's D = 0.75).

Taken together, our results suggested *H. neanderthalensis* potential range crumbled into a number of little-connected optimal patches, which means its population was steeply reducing in numbers and growing in isolation before its extinction. The intensity of these patterns is higher at 44 and then at 40 ka, a period almost coincident with a sudden, global climatic shift towards colder temperatures linked to Heinrich Event 4. These findings perfectly fit with the results found in Raia et al. 2020. Climate change play a key role for Neanderthal's extinction. We observed a contraction of its geographical range size toward regions characterized by less harsh climatic regime for the species. Unsurprisingly, fossil record suggested a progressive retreatment toward southernmost areas and the simultaneous depopulation of mountain and continental area characterized by high seasonal climatic regime (Benito et al. 2017).

In term of landscape structures, the high fragmentation of predicted distribution lead to demographic and genetic negative consequence. Neanderthals were found to have had small population size and high mortality rates before their extinction. This demographic instability combined with the fragmentation of geographical areas and variations in their distribution and extent could have represented a primary factor for Neanderthal's demise (Bocquet-Appel & Degioanni, 2013; Sørensen, 2011). It is been demonstrated fragmentation of natural habitats is associated to population declines of many species. Small and isolated populations are more vulnerable to demographic and environmental stochasticity. They also face several genetic threats. First, due to restricted mating opportunities, inbreeding becomes more likely (Keller &

Waller, 2002). Second, if populations remain small and isolated for many generations, they lose genetic variation necessary to respond to environmental challenges (random fixation or loss of alleles through genetic drift). Third, unfavorable mutations are expected to accumulate because genetic selection operates less efficiently in small populations. Consequently, environmental, demographic, and genetic factors can interact and reinforce each other in a downward spiral, known in ecology as "extinction vortex" (Blomqvist et al. 2010).

Our results reinforce the primary role of climate changes for Neanderthal's demise. On the other hand, the high degree of climatic niche overlap does not exclude a direct competition with *H. sapiens* even if we are far from considering it a primary role for Neanderthal's extinction. Our results suggest a synergic action between climate conditions and *H. sapiens* competition which became stronger after 45 ka, a temporal period when the climatic regime became very harsh and the colonization of Europe by *H. sapiens* was complete.

Recent works on human genomic demonstrated *H. neanderthalensis* and *H. sapiens* populations even interbred among them. Green et al. 2010 compared Neandertal genome to the genomes of five present-day humans from different parts of the world showing that Neandertals shared multiple genetic variants with present-day humans (Green et al. 2010). Fu et al. 2015 estimated 6-9% of DNA belonging to Peştera cu Oase individual, one of the more archaic European specimens ascribed to *H. sapiens*, derived from Neanderthals. Furthermore, the authors estimated Neanderthals have contributed 1–3% of the DNA of present-day people in Eurasia (Fu et al. 2015). Subsequent works focused on the effects of the introgression of the Neanderthals genome. Dannemann & Kelso 2017 found Neanderthal DNA is involved in skin tone and hair color, height, sleeping patterns, mood, and smoking status in present-day Europeans (Dannemann & Kelso 2017), while Sankararaman and colleagues argued high frequency of Neandertal alleles in modern humans are enriched for genes affecting keratin filaments suggesting they may have helped modern humans adapt to non-African environments (Sankararaman et al. 2014). Unfortunately, Neandertal DNA seems to cause more vulnerability to several disease traits, such as neurological traits, autoimmune diseases, prostate cancer, and type 2 diabetes (Dannemann 2020).

***Homo sapiens* and Megafauna**

The last part of this thesis focusses on relationship between *Homo* and Quaternary megafauna. To better understand the mechanisms that ruled the ecosystem functioning within the mammal paleo-communities, in Mondanaro et al. 2017, we investigated the trophic relationships between Neogene mammal species belonging to different trophic categories. The results of this article suggested a constant top-down control of megaherbivores in mammal communities. Specifically, when megaherbivores were present in the ecosystems, the biomass available to carnivores reduced, exactly because megaherbivores are hard to kill, and smaller herbivores were significantly outcompeted (and their population size thereby decreased) by the larger herbivores. This phenomenon translates in a double negative effect for diversity of mesoherbivores due to role of both carnivores and megaherbivores. Consequently, predation and direct competition increase extinction risk in small herbivores, as often suggested to occur for living prey species (Fritz et al. 2002; Malhi et al. 2016).

Taking in mind these findings, I restricted the spatial scale of my research to Late Quaternary megafauna extinction. This is still one of the most debated topics in scientific literature. Multiple explanatory hypotheses for this global extinction event have been proposed, including climate change (Wroe & Field 2006; Guthrie 2003), the spread of *Homo sapiens* on global landscape and related effects of hunting and habitat change (Burney & Fannery 2005), even an extra-terrestrial impact (Firestone et al. 2007), and hyper-disease (Lyons et al. 2004). However, only two of these hypotheses have received broad support as the primary drivers of megafauna extinction even if their absolute and relative importance remains a contentious issue. Moreover, the question has increased over time because it been demonstrated the different role of both human activity and climate change at different spatial and temporal scales. In one of the most famous articles about this topic, Sandom and colleagues quantified the effect of human and climate change in many continental areas. The authors found a strong correlation between hominin palaeobiogeography and regional extinction ratios of mammal species in Americas and Australia. In contrast, the magnitude of this phenomenon was minimal in Africa continent, whereas the *Homo* activity alone failed to explain the high extinction rates of megafauna species in Eurasia during the Late Quaternary (Sandom et al. 2014).

Subsequent articles supported the human-driven megafauna extinction proving the "overkill hypothesis" at local scale (Martin 1973). In according to Martin's idea, human appearance and subsequent hunting of local megafaunal mammals fueled rapid human population growth resulting in both the colonization of landscape and the extinction of almost megafauna species. Surovell et al. 2016 tested the overkill hypothesis in Americas where 38 genera of large mammals became extinct during a narrow time interval of the Late Pleistocene, between 12-14 ka ago (Surovell et al. 2016; Faith & Surovell 2009). This narrow time period also encompasses the Younger Dryas cold interval (Alley 2000; Rasmussen et al. 2006) and the arrival of Clovis hunter–gatherers, for a long time considered the first human populations peopling the North America (Waters & Stafford 2007). In this delicate matter, Surovell and co-authors demonstrated a temporal overlap between human arrival into New World and the decline of extinct megafauna species. This temporal pattern occurs first in eastern Beringia, next in the contiguous United States, and last in South America (Surovell et al. 2016; Johnson et al. 2013). However, new anthropological evidences and advances in method and calibration dating (Reimer et al. 2020) allowed a more-defined reanalysis of human-driven hypothesis about megafauna demise in Americas. Many authors traced back the arrival of *Homo sapiens* in North America before Clovis era documenting the human use of both stone and osseous tools by Pre-Clovis populations (Waters et al. 2011, 2018; Halligan et al. 2016). And on the top of this, recent works on DNA contained in human coprolites supported pre-Clovis human occupation (Shillito et al. 2020). These new findings suggested population dynamics of humans in Americas predated the beginning of LGM. If new evidences are confirmed, they could demonstrate a long-term interaction between humans and megafauna and a necessary revaluation of human-driven hypothesis.

Similar considerations were demonstrated for Australia, where mounting evidence points to the loss of most mammal species before the human peopling of the local landscape and a significant role for climate change in the disappearance of the local megafauna (Wroe et al. 2013), even if for many islands of Oceania, the Holocene arrival of humans correlates closely with the timing of megafaunal extinctions (Holdaway et al. 2014; Perry et al. 2014).

I faced this delicate matter focusing on Eurasian continent where the debate about the causes of megafauna extinction is still unresolved (Price et al. 2018). The debate is exacerbated by observation of a more protracted

temporal co-existence between human and megafauna compared to Americas and Oceania. Taking it in mind, many authors turned to ecological disturbance caused by both human activity and climate changes rather than limiting their studies to chronological coincidence of human arrival and megafaunal extinction. Many works evaluated the human impact in term of habitat alteration and trophic disruption rather than analyzing the active role of human hunting (Ripple & Van Valkenburgh 2010) Following this trend, recent studies estimated the magnitude and speed of climate changes during the Late Pleistocene in order to evaluate their impact on physiologies, adaptations, climatic tolerances, competitive interactions related to megafauna species, understanding what led to their extinction (Mann et al. 2019; Botta et al. 2019), even if large-scale investigations on Pleistocene ecosystems are rare.

In ("*The well-behaved killer: Late Pleistocene humans in Eurasia were significantly associated with living megafauna only*"; Carotenuto et al. 2018), we tested the direct role of human hunting considering simultaneously the climatic preferences of both human and their potential prey species. This is because species with similar climatic requirements tend to coexist, and a correct evaluation of the potential impact of hunting on prey populations depends on prey availability to the hunters (Lorenzen et al., 2011). We predicted the megafauna and *H. sapiens* occurrence probability maps over the last 40 ka in Eurasia by using Species Distribution Models (SDMs). After that, we used SDMs output to ascertain which potential prey species were abundant where humans occurred the most. In according with overkill scenario, the distribution of optimal habitat patches for humans must overlap with that of the extinct megafauna. In contrast, humans might have been alternatively associated with different prey species in keeping with changing climatic regimes, which would suggest they had the potential to exploit different game species at different times.

For our purpose, we built a faunal database with 4965 Eutherian mammal occurrences distributed over 749 eurasiatic fossil localities for 24 either extinct or extant species belonging to the orders of Artiodactyla, Carnivora, Perissodactyla and Proboscidea. Moreover, we collected the eurasiatic human occurrences dated before 40 ka included in the Canadian Archaeological Radiocarbon Database (CARD; Gajewski et al. 2011). Following the same criteria described in Mondanaro et al. (2017), we partitioned mammal species into different trophic groups according to their body size, feeding category, and status setting eight ecological categories:

'Extinct Large Herbivores', 'Extinct Medium Herbivores', 'Extinct Large Carnivores', 'Extinct Medium Carnivores', 'Extant Large Herbivores', 'Extant Medium Herbivores', 'Extant Large carnivores' and 'Extant Medium Carnivores' (Mondanaro et al. 2017). To assess the influence of human activity on mechanisms of ecosystem functioning during the Late Pleistocene, we used ecological groups in order to quantify their geographical overlap with *H. sapiens* range.

To perform SDMs, we used the same climatic dataset described for Melchionna et al. 2018 (see above) obtaining the climatic values related to both mean temperature and precipitation of warmest and coldest quarter, respectively (Singarayer & Valdes, 2010; Melchionna et al. 2018).

To calibrate SDMs, we first divided the fossil record of both humans and large mammals into successive 4 ka long time bins and then we followed the same procedure described in Raia et al. 2020 and Mondanaro et al. 2020 to generated 10.000 background points over Eurasia. We accounted for age uncertainty without the use of 100 replicates, as described in Raia et al. 2020. In this case we adopted a temporal moving window approach to solve the potential issues linked to fossil localities age uncertainty (see below).

For each 4 kyr long time bin, we extracted climate data at each occurrence and background point and repeated the procedure described in Melchionna et al. 2018 to apply an ensemble forecasting approach, as implemented in the biomod2 package. Specifically, we chose to test the same four different algorithms (i.e., GLM, GAM, GBM, MAXENT) and used the same cross-validation design. To avoid using poorly calibrated models, only the projections from the models with AUC > 0.75 were considered in the subsequent analyses. Models were averaged calculating a weighted mean by model's AUC (Melchionna et al. 2018). Finally, continuous model projections were transformed into binary, presence/absence maps, using the threshold that maximizes the sum of sensitivity and specificity (Maiorano et al. 2013).

Then, we used the trophic group affiliation as the response variable in a multinomial logistic regression model, whereas as explanatory variables, we considered the following five covariates derived from the SDMs output:

1) Climatic plasticity (Figure 7b). It indicates if a species occupied similar climates under constant climatic conditions (high climatic conservatism) or, alternatively, the species tend to search constant environmental conditions under climatic change (i.e. high climatic plasticity in our sense).

2) Total area of the species most suitable territories ("PIXEL95", Figure 7C, the total geographic area where the habitat was highly-suitable for the focal species). PIXEL95 counts the number of pixels above the 95th percentile of the suitability distribution for the focal species. Therefore, it represents the total area where the species is presumed to be abundant.
3) The mean suitability value of the focal species ("PIXEL95H") within *H. sapiens* PIXEL95 (Figure 7D).
4) Degree of geographic overlap (OVERLAP, Figure 7E) between the focal species and *H. sapiens* in terms of predicted suitable areas. This was calculated as the ratio between the count of pixels shared by both the focal species and *H. sapiens*, and the total count of pixels obtained by combining the maps of the two.
5) Range shift over time (DISTANCE, Figure 7F) is the extent of range shift over successive time intervals. DISTANCE is calculated as the Euclidean distance between the centroids of species predicted ranges over consecutive time bins. Centroids were located by weighing the suitability values predicted within the species range per time bin.

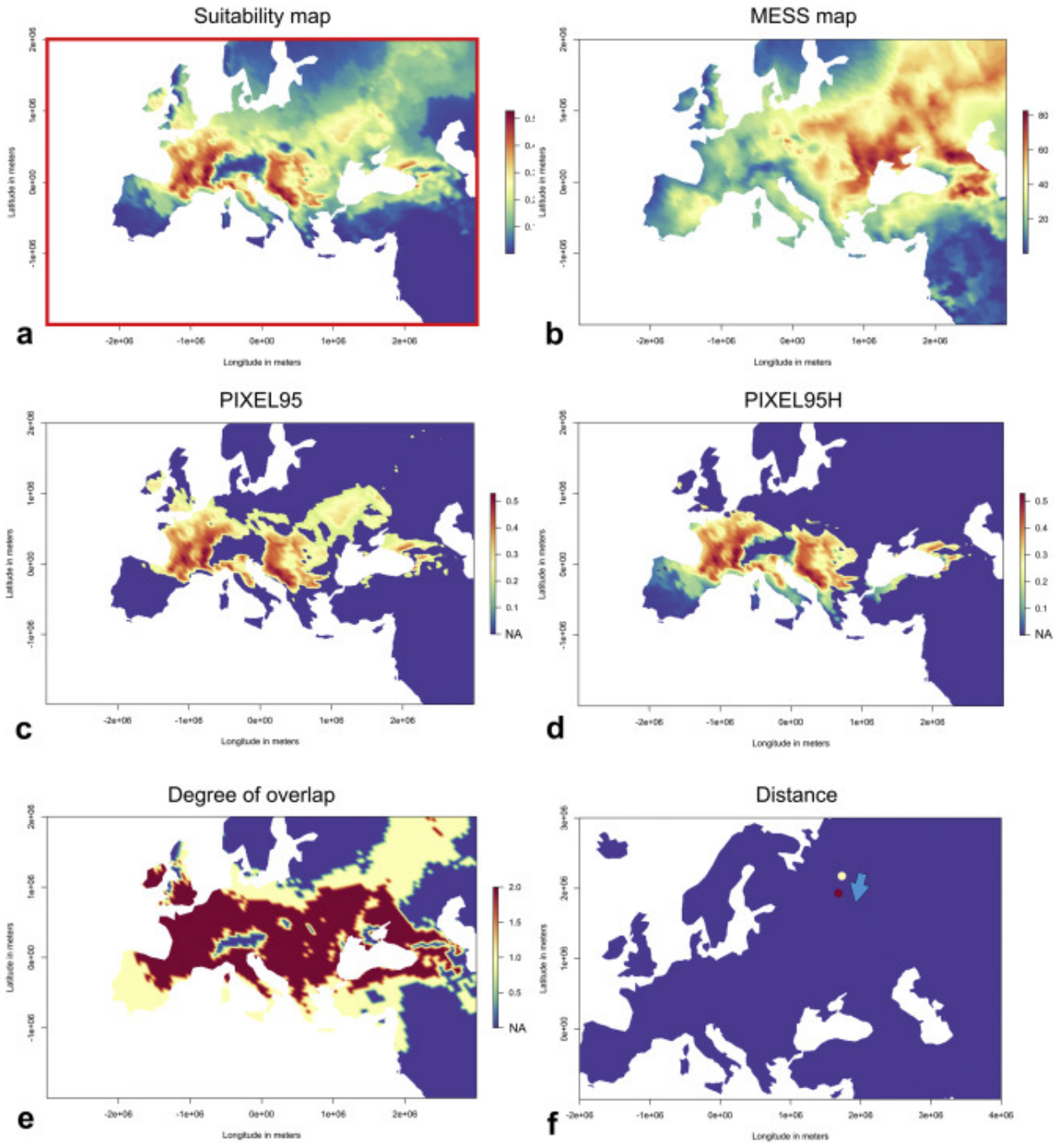

Figure 7. A) Suitability map of the wholly mammoth during the Last Glacial Maximum (~24 ka) as an example. Colour gradient indicates increasing values of suitability from the lowest (violet) to the highest (red). All the other variables were derived from this map. B) CLIMATIC PLASTICITY of the species. C) PIXEL95 is the map showing suitability values higher than the 95th percentile for the considered species. D) PIXEL95H is the map of species suitability values included in the space delimitated by the *Homo sapiens* PIXEL95. E) Map showing the degree of overlap between the predicted distribution of *H. sapiens* and the wolly mammoth. Red pixels

indicate the geographical overlap, yellow values indicate not-overlapping regions and violet pixels indicate no predicted geographic distributions. F) Map showing wolly mammoth's distribution centres in two consecutive time intervals. The yellow point indicates the distribution centre during ~28 ka and the red one indicates the distribution at ~24 ka. The arrow indicates the computed Euclidean distance between the two centres. Image from Carotenuto et al. 2017.

The regressions were computed over consecutive time bins, but they were repeated applying the temporal moving window approach. Specifically, we took predictors averages computed over three consecutives, overlapping temporal intervals. This procedure allowed us to create new predictor maps each one averaged over three original consecutive ones, except for the penultimate interval, whose moving window spans over two intervals only. By using this approach, we calculated multinomial logistic regressions on the entire species pool, and then by testing herbivorous and carnivorous taxa separately.

To assess spatial association between mammal fauna and *H. sapien*s, we calculated statistical relationships between *H. sapiens* suitability values inside its PIXEL95 map and the corresponding suitability values of each mammal species inside PIXEL95H, averaging suitability values over all time bins. After that, we applied linear regressions both univariate (i.e., species by species) and multivariate (all herbivorous species together), to explore whether *H. sapiens* was associated to different mammal species under different climatic conditions. We ranked species by partial regression coefficients, and applied Wilcoxon Signed-Rank test comparing pairs of consecutive bins for the identity (and rank) of the species most associated to *H. sapiens*. This statistical test verifies whether the rank-suitability distribution of species within the predicted human range did change passing by time interval to another.

Regression outputs suggest extinct large herbivores presented higher geographic range overlap with *H. sapiens* compared to other trophic categories. (Figures 8a-b). Since megafauna extinction has mainly affected large-bodied mammals, regression results indicate humans theoretically had very good chance of encountering the extinct megafauna, in keeping with the overkill hypothesis. However, once we performed regressions by using only herbivore as response variable, extant medium-sized herbivores showed significantly higher values

of suitability than extinct large herbivores within the core of human distribution (i.e., PIXEL95H, Figure 8b). Consequently, we can assume extant medium-sized herbivores were abundant where also humans were more abundant in according to habitat suitability values. Although we found a significant correlation between large extinct herbivore and human habitat in term of overlap, archeological evidences for direct killing of large prey like mammoths and elephants are rare in fossil record (Gaudzinski et al. 2005) documenting only an exploitation of proboscidean carcasses at most (Shipman 2015). In contrast, archeological record indicates that medium-size herbivore (i.e., deer, auroch, and wild boar) were humans' preferred preys (Stewart 2004; Stiner & Kuhn 2006).

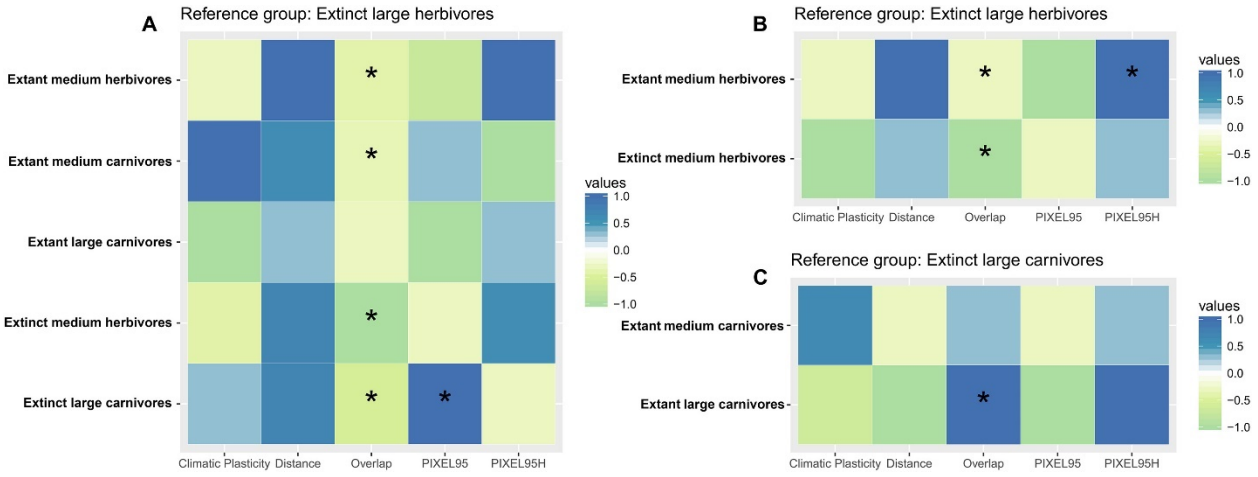

Figure 8. The relationship between humans and different ecological groups of the a) entire megafauna, b) herbivores and c) carnivores analyzed separately. In blue tones, the focal ecological group has higher values than the reference group, the opposite applies to green tones. Image from Carotenuto et al. 2017.

These results suggest a form of prey selection in which humans selected the most abundant prey occurring in their habitat. Furthermore, the rank abundance analysis demonstrated the available spectrum of prey species changed over time in according to climate changes. For instance, we can observe a close association between human and the cold-adapted mammal species during the Last Glacial Maximum (LGM), whereas we found a clear relationship between human and warm-adapted species during the subsequent period of deglaciation. Interestingly, such strong climatic tolerance is been demonstrated for carnivorous mammals, and might explain

the positive relationship between humans and extant large carnivores (8a-c). This is further supported by the evidence that extant carnivores might have overcome end Pleistocene extinction by virtue of such wide climatic tolerance (Di Febbraro et al. 2017). In contrast, the low overlap between extinct large carnivores and human range suggests they might have gone extinct primarily by climatic effects. Our findings suggest mammal species with high extinction risk were not the targeted species of human hunting. This suggestion corroborated the idea that *H. sapiens* was not the main factor for Eurasian megafauna extinction, although it is still possible that human exploitation contributed to amplify the vulnerability of some taxa to climate change.

I published a second work related to the topic of megafauna extinction. In ("*Additive effects of climate change and human hunting explain population decline and extinction in cave bears"*; Mondanaro et al. 2019), we performed a population viability analysis (PVA) on *Ursus spelaeus*, an iconic component of megafauna, to investigate about the cause of its demise during the Late Quaternary. PVA is a powerful tool very used in conservation biology and even sponsored by International Union for Conservation of Nature (IUCN) to predict species demographic evolution and extinction risk forward in time by taking into account the species' vital rates and the incidence of catastrophic events (Aiello-Lammens & Akcakaya 2017). PVA is able to consider the constituent populations of a single species (its metapopulation) as an interconnected, dynamic unit and to work in a spatially explicit context. In this article, we applied for the first time PVA to an extinct species to elucidate which combination of factors and parameters best explains the estimated *U. spelaeus* extinction date at 24 ka (Baca et al. 2016; Terlato et al. 2018), and to show that PVA is a powerful method helping to understand the determinants of extinction in fossil species.

We estimated the carrying capacities and vital rates of cave bear population and analyzed their temporal variation over time. PVA forecasts the demography of the species thereby assessing extinction risk in the future. In this article, we reverse-engineered PVA to select the best-model that explains the extinction of *U. spelaeus* according to a specific target at a given time, that is a total population of only 100 female individuals still alive at 24 ka (i.e. the last occurrence date reported for *U. spelaeus*). We did not set the target at zero individuals because species extinction dates in the fossil record most likely pre-date the real extinction of the species in according with the Signor–Lipps effect (Signor & Lipps 1982). By the same reasoning, models predicting the

extinction before 24 ka were considered unfit, as the species was still extant at least until that moment.

For our study, I collected during my doctorate 138 fossil occurrences belonging to *U. spelaeus* covering the 72–24 ka timespan. After that, we used the climatic variables generated in Singarayer and Valdes 2010 in order to perform species distribution models (SDMs) on cave bear. To calibrate SDMs, we followed the entire procedure described in Melchionna et al. (2018). SDM outputs gave habitat suitability maps for cave bear over the timespan 72 to 24 ka and updated every 4 ka in according to temporal resolution of climatic dataset (Singarayer & Valdes 2010). Model projections were then transformed into binary maps using the threshold that maximizes the sum of sensitivity and specificity (Di Febbraro et al. 2015; Maiorano et al. 2013).

As subsequent step, we developed a spatially explicit metapopulation model for *U. spelaeus* including female individuals only. The starting data selected were (i) initial abundance, (ii) carrying capacity (K), (iii) stage structured matrix with survival and fecundity per age class, (iv) density dependence mechanism for population growth, and (v) environmental and demographic stochasticity.

Population size estimation using the cave bear genome shows that during the Late Pleistocene the effective population size (Ne) was around 10 000 individuals (Stiller et al. 2010; Ho & Shapiro 2011). Since the Ne is generally close to one-quarter of the total population (Lande & Barrowclough 1987), and considering that we decided to model females only, we set the initial abundance at 20 000 cave bear individuals. As regard the carrying capacity, we imported the *U. spelaeus* binary maps produced by the SDMs into RAMAS GIS software (Akcakaya & Root 2013) to determine the spatial structure of the metapopulation. After that, we considered suitable cells separated by a distance less than or equal to 150 km from each other (neighbourhood distance = 3 cells; Anderson et al. 2009) as unique populations. We linked the metapopulation model to the habitat suitability maps by defining a specific value of K for each time interval. Specifically, we calculated K for each patch as follows (1):

$$\text{Equation 1:} \qquad K_i = ths_i * 0.02 * 2500 \quad (1)$$

where K_i represents the carrying capacity during the $_i$th time interval; ths_i is the sum of habitat suitability values of each patch in the $_i$th time interval; 0.02 is the *U. arctos* population density*km^2 retrieved from the PanTheria database (Jones et al. 2009); and 2500 is the area of each cell (in km^2).

To construct a stage-structured model, we designed a Lefkovitch stage-structured matrix (Lefkovitch 1965) in which we defined three age classes: cubs, juveniles (1–4 years old individuals below sexual maturity), adults (potentially breeding individuals). We decided to retrieve the fecundity and survival data from recent studies about the Italian brown bear (Gervasi et al. 2011; Gervasi & Ciucci 2018) because several studies show that *U. spelaeus* and the living *U. arctos marsicanus* shared similar morphological and ecological adaptations (Stiner et al. 2016; Loy et al. 2008). Moreover, we set all vital rates and stage classes as subjected to density dependence mechanism selecting the ceiling density dependence function in which the population grows exponentially until it reaches K. To take into account uncertainty associated to each demographic parameter (fecundity and survival), we built for each of them a distribution having the designed parameter value as the mean and a specified standard deviation around it. As for demographic parameters, we used the standard deviations of *U. arctos marsicanus* parameters reported in Gervasi et al. 2011 and Gervasi & Ciucci 2018. This procedure allowed us to incorporate a demographic stochasticity by randomly varying the (integer) number of survivors and cubs for each stage. For each spatially explicit metapopulation model, 10 000 iterations were run picking values at random from the statistical distributions of starting values.

We designed six possible extinction scenarios alternatively simulating the effect of climate change, *H. sapiens* presence and their combination over 52 thousand years of *U. spelaeus* evolution, up to the actual extinction record at 24 ka (Baca et al. 2016). Each simulation was run with 10 000 iterations using starting demographic values and their standard deviations to account for parameter uncertainty.

In our models, climatic variation influences population size, carrying capacity and vital rates via the link between SDM-derived suitability values and metapopulation size and spatial configuration. The influence of *H. sapiens* was modelled as a reduction in survival, regardless of the age class partitioning. Particularly, variation in survival was included as a vector of multipliers that modifies the survival parameters of the stage matrix for the related timestep (e.g. a multiplier of 0.8 will reduce the survival by 20% for the focal timestep). The vector of multipliers was as long as the number of timesteps in the simulation. For time bins in which *H. sapiens* was not widely widespread present in Europe (i.e. before 40 ka, Benazzi et al. 2011), there is no influence on survival rate, so that the multiplier is set to 1. Survival multipliers are free parameters. For this reason, we had to explore the

best-fit parameter combination by performing randomization procedures.

The first model ignores the effect of both climate change and human presence on cave bear demographics altogether, therefore K is computed for the first timestep only and remains constant over the subsequent timesteps, whereas *H. sapiens* influence is not considered. As carrying capacity is linked to habitat suitability, this is equivalent to assuming that climatic change effects are ignored altogether.

The second model accounts for the climatic change effects only. K-values are computed following Equation 1 for each timestep. *H. sapiens* influence on survival rates is ignored. Under this scenario, we were able to evaluate the influence of climate on cave bear metapopulation evolution on its own.

Model three and four consider only the detrimental effect of *H. sapiens* (starting at 40 ka) on bear survival proportional to either a linear increase of human population size through time (Bocquet-Appel & Demars 2000) or randomly variable human effects through time. To explore this effect, we created 1000 vectors of multipliers for each of two different model types, 'linear' and 'random'. In the 'linear' models, the initial (at 40 ka) human effect is picked at random a mere 5 up to 50% reduction in survival. Whatever the initial parameter is, the negative survival effect is then increased by 5% at each timestep. The increase is meant to capture the impact of a linearly increasement of *H. sapiens* population size and technological ability of time. For instance, following this model, we assume that *H. sapiens* is 20% more influential on bear survival at 24 ka than at 40 ka. In the 'random' models the 1000 vectors of multipliers were built by randomly picking values from a uniform distribution ranging from 0.5 to 0.95. This means that there is no direct connection between *H. sapiens* population size and bear survival. For each vector (either linear or random) 10 000 iterations were run using starting demographic parameters and their standard deviations. In both cases (i.e. linear and random) the best-fit survival vector was found by comparing to each other all the vectors producing an estimated population size between 95 and 105 individuals at 24 ka. In fact, as we have said above, we consider a value of 100 female individuals as the minimum viable population (MVP) for the cave bear. This means that we considered the species extinct in the timestep that got closest to 100 individuals.

We performed two last models combining both the effect of climatic change and *H. sapiens* pressure. In these model K is computed according with the Equation 1. *H. sapiens* influence is modelled through 1000 different

"linear" vectors (see above) in the fifth model, whereas we used 1000 different "random" vectors (see above) in the last scenario.

Once the best-fitting model from each scenario had been calculated, we assessed its sensitivity to different values of abundance, stage-specific survival rates and fecundity following the approach described in Aiello-Lammens & Akcakaya (2017). We applied a variation of ±10% on each of the starting parameters of each model. We sampled 1000 random combinations of initial parameter values from the distribution for each parameter (i.e. the starting parameter ±10%) to run 10 000 new iterations for each combination and for each model. After running simulations, we retrieved means and confidence intervals around the means to establish the terminal extinction risk (i.e. the probability that the metapopulation will end up below a certain population level at the end of the considered time-span) for the *U. spelaeus* metapopulation at 50, 100, 250 and 1000 individuals at 24 ka.

PVA forecasts demonstrated a surprisingly large effect of climate change starting at 40 ka. The second model shown *U. spelaeus* experienced a 10-fold decrease in population size passing through the 40 to 36 ka time interval even ignoring *H. sapiens* presence (Figure 9). Intriguingly, the 40-36 ka time frame immediately follows two important cold shifts in global temperatures, known as Heinrich events (H5 and H4; Marshall & Koutnik 2006), which suggests a causal relationship between the population decline after 40 ka and climate change. However, despite the intense effect of climate on cave bears' survival, PVA surprisingly found it fails to explain the extinction of the cave bear. Sensitivity analysis suggested that changing the starting parameter values combination by as much as 20% around each parameter the climate-only model (model 2) in the worst-case scenario still has 0.009 probability of the cave bear population having 100 female individuals only at 24 ka.

Models ignoring climatic effects and considering only *H. sapiens* did not drive *U. spelaeus* to extinction (Figure 9). Only the combination of climatic drive and *H. sapiens*' arrival is able to predict *U. spelaeus*' extinction at 24 ka (Figure 9). By analyzing the extinction risk at 24 ka, the probability that the species goes extinct (i.e. reduces to 100 individuals) with these models is some 60% (Figure 10). By changing the initial parameter values, the composite models (models 5 and 6) still predict a probability of reducing the cave bear population to 100 female individuals at 24 ka in the 30 to 90% range (Figure 10). In contrast, the probability is close to zero for models 2

and 3 (Figure 10). Interestingly, amongst the simulations working with temporally variable (random) *H. sapiens* effects on cave bear survival, the best iteration selected coincides with a progressive increase of the detrimental effect of *H. sapiens*, starting with a meagre 10% reduction in bear survival at 40 ka.

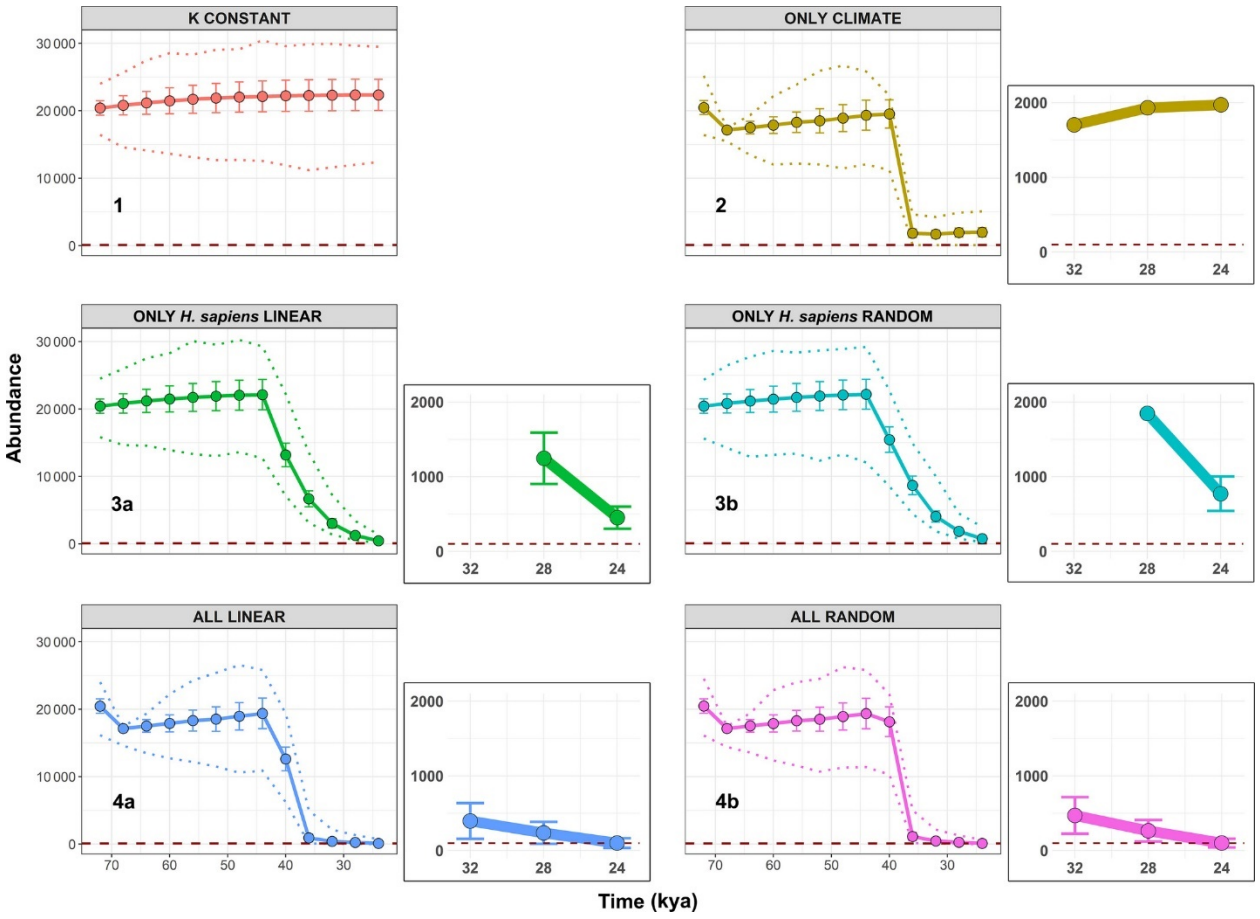

Figure 9. Trajectory summaries. Lines depict the number of individuals per timestep of the *Ursus spelaeus* metapopulation, under the six different geographically explicit PVA models. The expanded views show a magnification of each trajectory for the last three timesteps (from 32 to 24 ka). The red horizontal dashed line in each image represents the 100-individuals population boundary. The error bars around the trajectories represent the 95% confidence intervals around the mean population abundance estimate per timestep. The dotted lines indicate minimum and maximum abundance values estimated during the simulations. Image from Mondanaro et al. 2019.

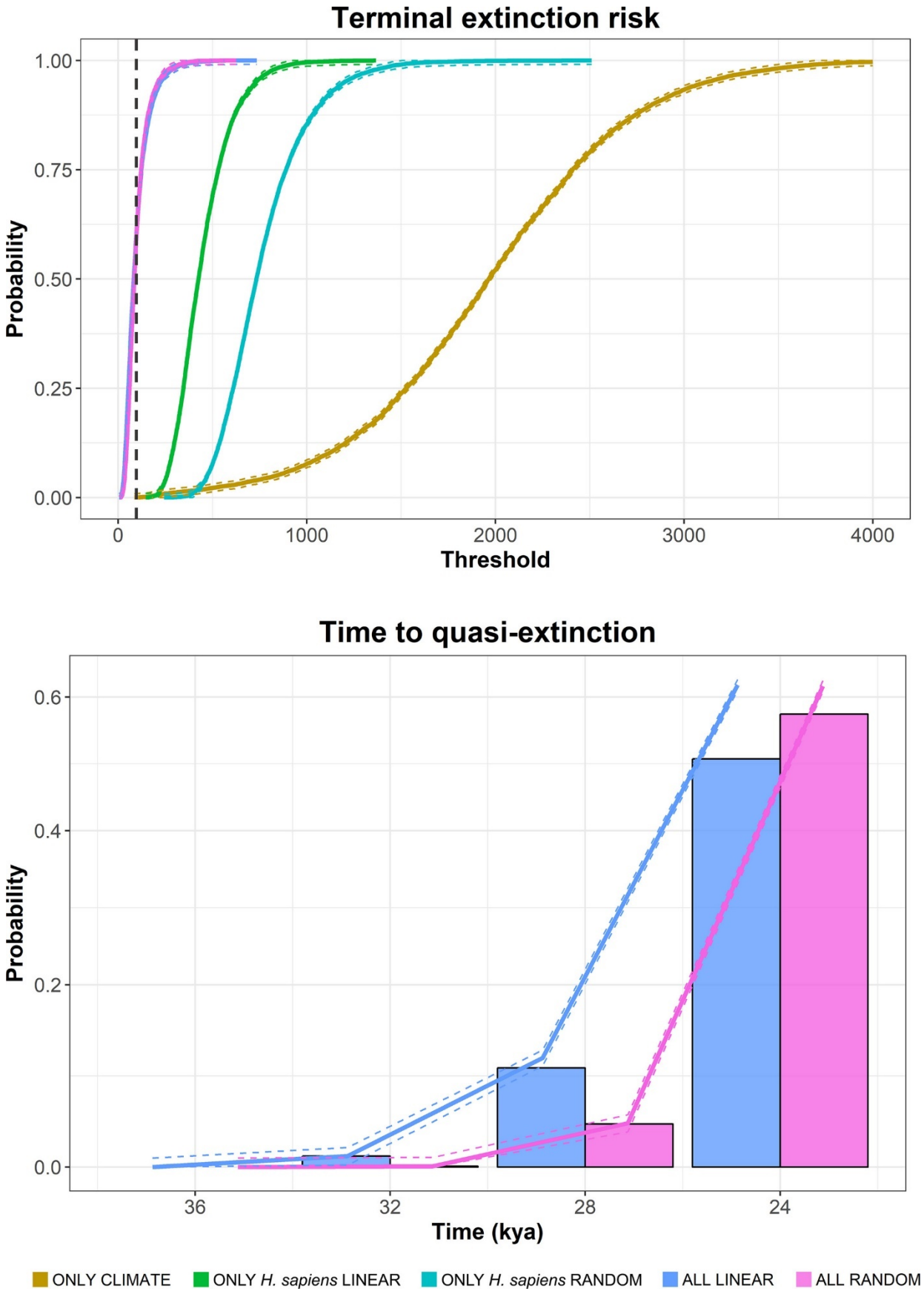

Figure 10. Extinction probabilities. Terminal extinction risk (top): y-axis, the probability of having a certain

number of individuals (x-axis) still alive at 24 ka for each model. Time to quasi-extinction (bottom): the probability that the *Ursus spelaeus* metapopulation went extinct per timestep (limited to the last four timesteps; only for models 5, 'linear' and 6, 'random'). Bars depict the quasi-extinction probability per timestep, while solid and dashed lines indicate the cumulative probability across the timesteps and their confidence interval, respectively. Image from Mondanaro et al. 2019.

From the biogeographical point of view, the decline of cave bear's population at 40 ka is likely linked to the appearance of two rare taxa within the cave bear species complex in eastern Europe, that is *U. kudarensis* in the Caucasus and *U. ingressus* in eastern Europe (Stiller et al. 2014) and the consequent retreatment of *U. spelaeus* range size towards westernmost areas of its geographical range (Figure 11).

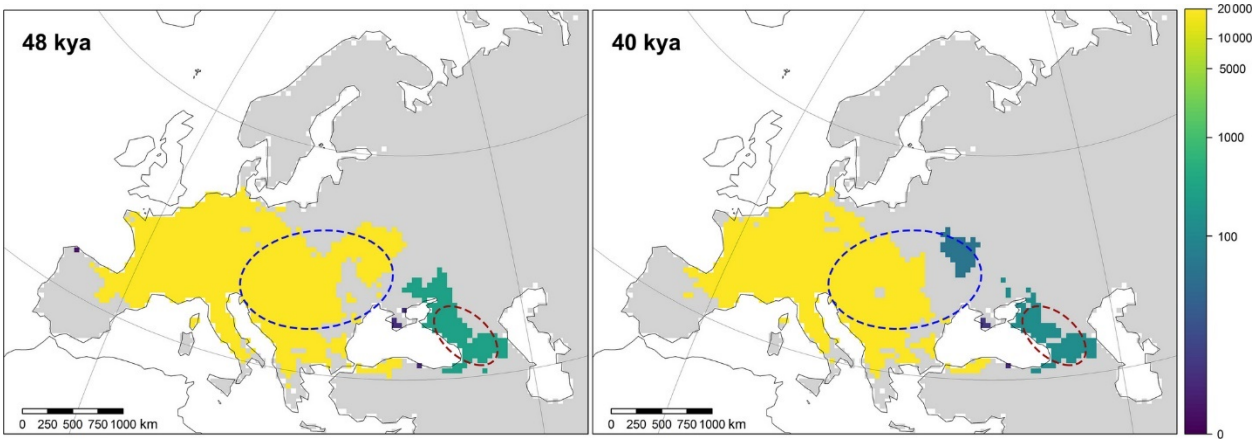

Figure 11. Distribution of cave bear populations at 48 and 40 ka as predicted by population variability analysis (model 5). Color gradient indicates abundance of individual populations (number of individuals) from low (purple) to high (yellow) values. The dashed lines indicate the geographical distributions of *U. kudarensis* (red) and *U. ingressus* (blue) following Stiller et al. (2014). Image from Mondanaro et al. 2019.

Comparing the model outputs, we observed the effect of *H. sapiens* on *U. spelaeus* survival was not dramatic, but, combined with climate change, it became nonetheless fatal. Our findings were a further evidence that climate change may be the main factor behind the dramatic megafauna population decline, rather than just being temporally correlated to it. Despite archeological records report direct evidence of bear exploitation by humans from several Upper Palaeolithic sites (Torres et al. 2007; Munzel et al. 2011; Baca et al. 2014;

Romandini et al. 2018; Terlato et al. 2018), these sites are younger than 45 ka, providing a further indication of the intensification of the negative effects of *H. sapiens* on cave bear viability occurred when cave bear population was already in decline. Hence, we suggest a combination of (primarily) climate change and (secondarily) human exploitation or indirect competition for space and resources (i.e. cave shelters; Grayson & Delpech 2003; Conard et al. 2006) is the best scenario for that *U. spelaeus* extinction.

Habitat fragmentation of megafauna species during the Late Quaternary.

As already mentioned before, large-scale investigations on Pleistocene ecosystems are extremely rare. We provide a first long-term study to investigate about the role of habitat spatial structure in species extinction. It is been demonstrated habitat spatial configuration affects species richness, abundance, and the chance for survival of wild species in the long run. Many researchers have given a central importance to habitat spatial structure for conservation planning and for landscape management. However, there still is a vigorous debate on the relative importance of habitat amount (total area of habitat) and habitat spatial configuration (the spatial arrangement of the habitat). Diamond (1975) first proposed on theoretical arguments that a single large area (SL) should hold more species than a number of small habitat patches amounting to the same total area. This idea attracted enormous interest, but at the same time generated the so-called SLOSS (single large or several small) debate. Some researchers criticized the lack of empirical and theorical studies in favor to Diamond's principle providing many ecological examples in favor to several small (SS) hypothesis (Gavish et al. 2011; Mac Nally & Lake 1999).

Many works pointed to integrate the Diamond's principle highlighting the necessity to consider such important factors as species overlap, minimum-area requirements, habitat diversity, and the distance between reserves for conservation planning (Soule & Simberloff 1986).

In the last decade, Fahrig (2013) fuelled the SLOSS debate by proposing the "Habitat Amount Hypothesis" (HAH). HAH states that species richness in a given sample site increase with the amount of habitat in the 'local landscape', defined as an area within an appropriate distance surrounding that site, with no additional effects of the size and isolation of the habitat patch in which the sample site is located. In accordance to HAH principle,

species richness is independent from the species spatial configuration. Particularly, HAH negates the fragmentation effect, which implies a decrease of species richness as consequence of the progressive subdivision of the species distribution into smaller, more isolated patches.

In a more recent article, Fahrig (2020) tested hers HAH theory on several SLOSS studies. In contrast to Diamond's principle, she found several small patches usually hold more species than few large patches of the same total area (SS > SL). She noted SS pattern held for specialist and threatened species, which suggests that the dominance of SS > SL is not a result of incursion by generalist species into small patches. Moreover, SS pattern does not change when natural of anthropogenic patches are considered.

Nevertheless, in a subsequent paper, Saura (2021) questioned Fahrig's findings. Following the HAH theory, Saura noted local landscape around the focal habitat site is defined by distance D (i.e. a circular area with radius D around the focal site). The value of D is not universal, but it is based on the focal site only.

Consequently, HAH predictions use the habitat amount in that local landscape to give predictions for that focal habitat site only, but they give incorrect species richness predictions in the rest of the habitat sites outside that local landscape. Without any assumption about D values, Saura demonstrated a strong influence of habitat spatial structure on HAH predictions. He found that the distribution of species richness, as predicted by the HAH, differs considerably across landscapes with the same total amount of habitat depending on habitat spatial configuration. Particularly, habitat fragmentation, while holding constant the amount of habitat, negatively affects the species richness in all or many of the habitat sites in the landscape. A similar pattern was detected when considering more elongated shape of the habitat patches (narrower patches), or larger perforations within the patches. Overall, size and shape of the patches can lead to declines in species richness in the landscape. Consequently, HAH predictions cannot extrapolate outside the focal habitat site and its relative local landscape because of limitation of scale effect (i.e. setting of D distance to define local landscape).

Fahrig continued the debate publishing a reply to Saura et al. 2021. In hers reply, the author partially confirms the scale effect limitation described by Saura arguing that the size and isolation of the patch containing a sample site only influence species richness at that site through their relationships with the amount of habitat in the site's local landscape. In other words, HAH suggests that the effects of local patch size and isolation on species

density at a site are both contained within the effect of habitat amount, and therefore the effect of habitat amount on species density at a site is stronger than the effect of local patch size, local patch isolation or their combination. Fahrig ends her reply stating HAH is equally compatible with either higher or lower species richness for a single large patch (or few large patches) than for several small patches with the same total area (SLOSS) but she stands on implication of HAH about the conservation planning. The author contrasts with the idea that "habitat fragmentation poses a threat to biodiversity, in addition to the threat posed by the loss of the total amount of habitat" (Saura 2021; Hansky 2015). She noticed this idea is incomplete and non-exhaustive in conservation. The level of habitat fragmentation per se cannot predict the loss of biodiversity at local site, while HAH can predict it by linking the loss of habitat amount to species richness.

Overall, SLOSS debate seems far from resolved. Such evidence has led to an expectation that there are predictable situations where the best strategy for conservation (i.e. SL or SS theory) depending on various factors (Fahrig 2020; Tjørve 2010; Pellettier 2000). One major limitation of SLOSS studies is that they fail to capture long-term effects on species persistence, by focusing on living wildlife and hence on the short temporal scale (Fahrig 2020). We provided the first long-term study on the importance of habitat spatial structure (as defined by patch size, number and degree of isolation) on species extinction, using the dense fossil record of Late Pleistocene large mammals of Eurasia, and fine detail paleoclimatic data. As mentioned before, the effect of *Homo sapiens* on its mammalian prey and competitors is possibly more intense where species were naïve to the new super-predator, that is in the Americas and Oceania Islands, whereas the signature of human effects is milder in Africa and Eurasia (where megafauna species and *Homo sapiens* had been in contact for long time) and possibly superseded by the contemporary effects of intense global climate change (Sandom et al. 2014; Carotenuto et al. 2016). However, large-scale investigations on Pleistocene ecosystems and their evolution are rare for Eurasia, despite the high-quality fossil record of most of the Eurasian continent. Eurasia thus offers the unique opportunity to test how the effect of geographic habitat structure on species survival changes through time. We applied SDMs and analysed landscape metrics for several different large mammal species lived in Eurasia during the last 200,000 years. We compared extinct to extant species landscape metrics asking whether the suitable habitat patches for extinct species were different, in terms of size, number and geographical

isolation, as compared to extant species.

We utilized a new implementation of GCM PLASIM-GENIE paleoclimate emulator (Holden et al. 2019). Specifically, monthly emulated paleoclimate variables at native climate model resolution (5°) were transformed into BIOCLIM anomalies and downscaled onto modern BIOCLIM observations (CHELSA, Karger et al 2017) at 0.5° spatial resolution using bilinear interpolation. Each variable was emulated fifteen times, and the mean values used for calculations that follow. Seventeen of the nineteen BIOCLIM variables (Karger et al 2017) were generated, omitting BIO2 (Annual mean diurnal range) and BIO3 (Isothermality) because the diurnal cycle was not simulated. Monthly mean temperature anomalies were applied for BIO5 (Maximum temperature of warmest month) and BIO5 (Minimum temperature of coldest month), assuming that temporal variability within each month is constant through time. Temperature anomalies were combined with the modern baselines additively. Precipitation anomalies were combined with baselines using a mixed multiplicative/additive approach (Holden et al 2019).

We used the fossil mammal occurrences collected during my doctorate. I built a mammal database revising and enriching the databases published in Carotenuto et al. (2016) and Raia et al. (2009).

For this work, I pruned my database to 31 mammal species belonging to the order of Artiodactyla, Carnivora, Perissodactyla and Proboscidea. For each occurrence, I recorded the georeferenced location, the stratigraphic context of the sample and its estimated age. Overall, the pruned database included 4496 mammal occurrences distributed over 802 fossil localities and 1082 geological or archeological layers.

Following the procedure in Mondanaro et al. 2020 and Raia et al. 2020, we accounted for the effect of dating uncertainty producing, around each age estimate, a uniform distribution bounded by the minimum and maximum dating error of each age. Then, we randomly sampled a single date within this distribution and repeated this procedure 100 times. The 100 resulting datasets were used in turn to calibrate 100 alternative SDMs. In addition, for each species and replicated dataset, we generated a separate set of 10,000 background points over Eurasia, which were used as pseudo-absences together with observed presences to calibrate the SDMs.

To account for potential sampling bias in occurrence data, we adopted a sampling strategy for pseudo-absences

that positively weighted their selection probability using a proxy of fossilization rate. Specifically, such proxy was obtained for each species from the density of its occurrence data (Phillips & Dudík 2008; Syfert et al. 2013; Roy-Dufrense et al. 2019) at 50-km2 grid cell resolution, calculated by pooling fossil data along all the time bins. Following the approach done in Fourcade et al. (2018) and Raia et al. (2020), we defined the background area using the species occurrences. Specifically, we obtained the convex hull surrounding all fossil localitites, then creating a buffer around it with a radius equal to 10% of the maximum distance between occurrences. The 10,000 pseudo-absences were subdivided across the time periods where each species occurred, proportionally to the number of fossil occurrences falling into each time interval. SDMs were calibrated using the maximum entropy modelling algorithm implemented in MAXENT version 3.3.3k ("dismo" R package; Phillips et al. 2006). Since it requires a robust parameter optimization step (Merow et al. 2013), we tested different MAXENT implementations through the "ENMeval" R package to find the settings that optimize the trade–off between goodness–of–fit and overfitting (Muscarella et al., 2014). Among the resulting parameter combinations, we chose the model reporting the highest area under the receiver operating characteristic curve calculated on the withheld data under cross-validation (AUC; Swets, 1988). SDMs were evaluated using a temporal block cross-validation approach, splitting data into 10 years temporal bins, which were in turn held-out from models' calibration and used to assess their predictive performance. Models were projected over Eurasia each 1000 ka, according to the temporal resolution of climatic predictors. In addition, we drop SDMs from dating replicates reporting AUC values <0.7, in order to avoid poorly calibrated models in the subsequent analyses. For each mammal species, we generated spatially-explicit predictions each 1,000 kyr time bin falling within temporal range of species occurrences in the fossil record. Model projections were binarized according to three threshold approaches (i.e. "equalize sensitivity and specificity," "maximize TSS," and "the 10^{th} percentile of predicted probability"; Liu et al. 2005), to account for the effect of using different binarization schemes (D'Amen et al. 2015).

In a similar way as done in Melchionna et al. (2018), we evaluated the degree of fragmentation between suitable habitat patches as predicted by SDMs at each time bin by calculating the following landscape metrics: Total area ("*lsm_l_ta*"), Number of patches ("*lsm_l_np*"), Mean patch area ("*lsm_l_area_mn*"), Mean Euclidean

nearest-neighbor distance ("*lsm_l_enn_mn*") and Aggregation index ("*lsm_l_ai*") as developed in the "landscapemetrics" R package (Hesselbarth et al. 2019).

Such metrics were calculated for each species, time bin, replicated date and binarization threshold. To describe the temporal dynamics of patches spatial configuration during the last 200 ka, we fitted linear mixed models (LMMs) where each of the abovementioned landscape metric was the response variable and the time, in kilo years (from 200 to 2 ka), was the explanatory variable. Response variables were first transformed using a logarithmic transformation as to improve their normality. In addition, since we were interested in testing for different temporal dynamics in patches spatial configuration of extinct and extant species, LMMs were fitted putting the "time" explanatory variable in interaction with the species status (i.e. extinct or extant). This setup allowed LMMs to fit two different landscape metric-vs-time relationships for extinct and extant species. As we did not have an a priori expectation about the shape of the relationship between landscape metrics and time (e.g. monotonic increasing/decreasing trends rather than one or multiple concavities), we accounted for possible non-linear patterns by fitting LMMs with linear, linear + quadratic, and linear + quadratic + cubic relationships. As to avoid overly complex models, LMMs including quadratic and cubic terms were compared with linear ones through AIC. To account for differences in metrics values among the different species, replicated datasets and binarization thresholds, we included such factors as random effects in LMMs, allowing the models to vary their intercepts accordingly. Models' goodness-of-fit was assessed by calculating the conditional coefficient of determination for LMM (R^2; Nakagawa and Schielzeth 2013). Furthermore, we evaluated LMMs by calculating their accuracy (i.e. correlation coefficient between the observed and the predicted value of the outcome) using a five-fold cross-validation scheme.

To assess the relative contribution of the landscape metrics, with respect of widely explored functional traits such as body mass and diet, in discriminating between extinct and extant species, we calibrated a Random Forest classification model (RF). In this model, we used the status of each species ("extinct" vs "extant") as the response variable, while the five landscapes metrics, body mass, diet and time in kilo-years were included as explanatory variables. Before applying RF mode, we run VIF analysis to select non-collinear predictors only (Zuur et al. 2010). We evaluated RF ability to correctly classify a species as extinct or extant according to the

abovementioned covariates by calculating the AUC under a five-fold cross-validation scheme. In particular, we optimally tuned RF settings by testing for different parameter combinations, then selecting the combination that yielded the highest AUC value. All RF candidate models were run allowing a maximum of 1000 trees. The optimal RF was then used to quantify the relative importance of each covariate within the classification model, as well as to generate partial effect plots depicting the shape of the relationship between the explanatory variables and the probability of a given species to be classified as "extinct", as fitted by RF.

Among the 31 modelled mammal species, 28 were retained for landscape dynamics analyses as they reported at least one replicated SDM with an AUC > 0.7 (excluding *M. primigenius*, *U. arctos* and *F.silvestris*). Overall, SDMs for these 28 species reached good to excellent predictive performances (sensu Swets 1988). For all landscape metrics, LMMs including linear, quadratic, and cubic relationships were ranked as the best ones according to AIC. Such models also achieved a high goodness-of-fit, with conditional R^2 values ranging between 0.432 to 0.825 (Table 1A). Aggregation index, Mean patch area, and Total patch area exhibited similar patterns in their temporal dynamics, though reporting different magnitudes between extinct and extant species. For extinct species, there was a substantial decline in the value of these three metrics between 200 and 150 ka (Fig. 12), followed by a turning point and significant upward concavities (i.e. cubic coefficients were all positive and significant; Table 1B) that led to subsequent increasing trends centered on the post-Eemian period (Fig. 12). The curves for these three metrics showed another turning point with a significant downward concavity (negative and significant quadratic terms; Table 1B) at around 70 ka (Fig. 12), then significantly decreasing toward present time. Linear terms coefficients were positive (see Table 1B) since LMMs were fit against the "time" explanatory variable ranging from 0 to 200 ka. That said, they can be interpreted as a decreasing temporal trend as we reversed the horizontal axis in Fig. 12 along the actual time direction. Temporal dynamics of Aggregation index, Mean patch area and Total patch area for extant species showed similar shapes to those of extinct species, although their fluctuations were less pronounced (i.e. coefficient magnitudes were a half to an eighth lower than extinct species; Table 1B). Temporal trends of Mean patch distance were markedly different between extinct and extant species. The former showed two upward concavities at ca. 120 and 80 ka, although only the second one was significant (cubic term=-0.361,

p=0.304; quadratic term=2.483, p<0.001; Table 1B). Moreover, the subsequent trend toward the present time is increasing though not significant (linear term=-0.637, p=0.065; Table 1B). On the contrary, extant species exhibited an initial drop in the value at ca. 150 ka, where a significant upward concavity occurred (cubic term=1.892, p<0.001; Table 1B). Subsequently, the metric had a keep increasing during the post-Eemian period until a second turning point, where a significant downward concavity (quadratic term=-0.963; p<0.001; Table 1B) led the curve to significantly decrease toward the present time (linear term=1.399, p<0.001). As for Number of patches, extinct species showed a significantly increasing trend up to the end of the Eemian period, where a significant downward concavity occurs (quadratic term=-20.516, p<0.001; Table 1B). From this point, Number of patches for extinct species decreases monotonically (linear term=12.792, p<0.001; Table 1B) toward the present time (Fig. 12). Extant species showed a rather different pattern, especially during the last 50 ka. In fact, the initial increasing trend reaches a significant tipping point with a downward concavity (quadratic term=-5.004, p<0.001; Table 1B) just before entering the Eemian period, then showing a substantially constant trend toward the present time (linear term=0.604, p=0.127; Table 1B).

VIF analysis forced us to exclude “total area” from the subsequent analysis. Once removed, RF model achieved a perfect ability to discriminate between extant and extinct species (AUC=1). In particular, the best-fit model (i.e. min.node size=1, mtry=6, splitrule= gini) reported a sensitivity = 1 and a specificity = 0.999. The variable importance associated to the optimal model showed a predominant role of body mass (some 52%). Landscape metric and diet split almost equally a further 40% of variance, (i.e. 18.03/26.73%), whereas the remaining model variance is explained by time (2.6%).

Marginal effect plots showed the probability to be “extinct” monotonically increased with lower values of aggregation index and mean patch area, and with higher values of body mass, mean patch distance, number of patches, and total area (Fig. 13). These results remain constant also when changing the time level (Fig. 13).

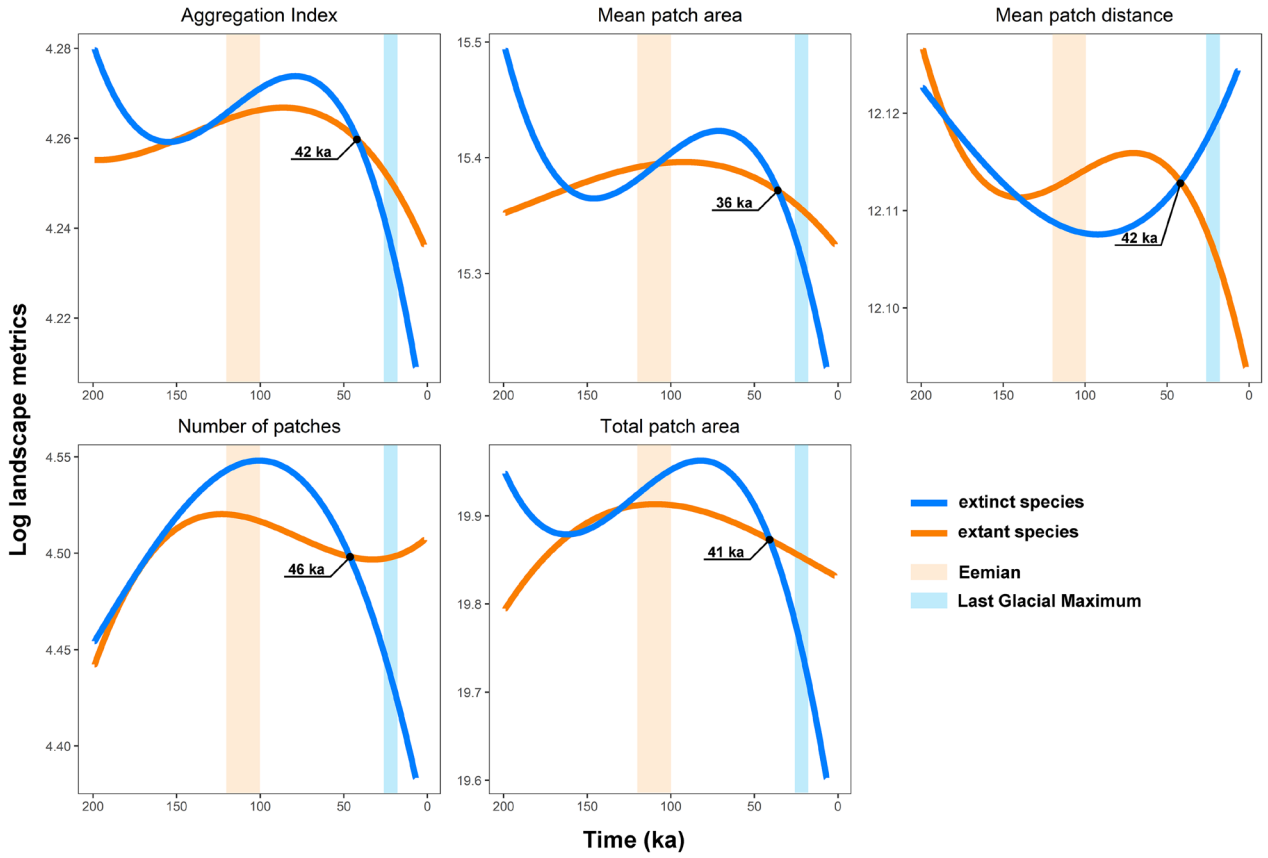

Figure 12. The relationship between landscape metrics (logged values) and time fitted by LMMs, plotted for extinct (blue line) and extant species (orange line). The vertical orange band highlights the Eemian period (120 to 100 ka), while light blue band highlights the Last Glacial Maximum period (26 to 18 ka).

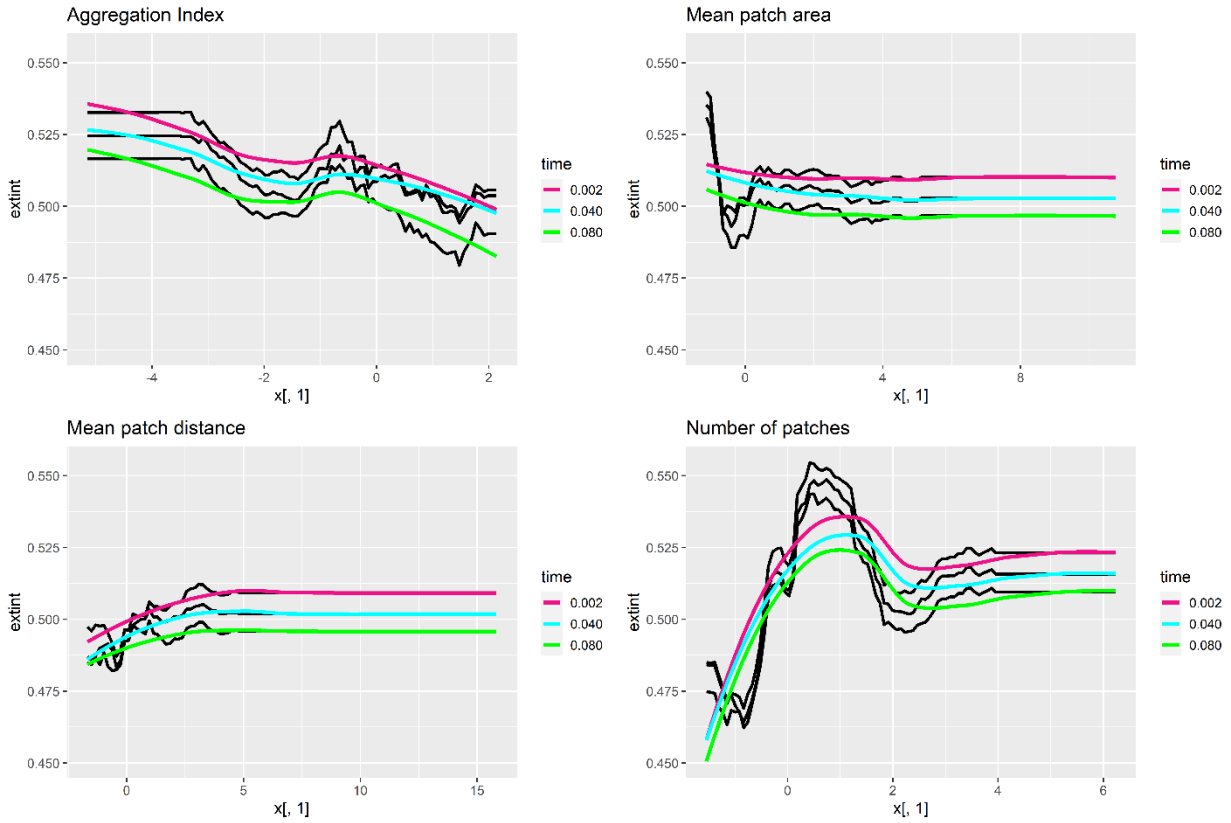

Figure 13. Marginal plots showing the shape of the relationship between the landscape metrics and the probability of a given species to be classified as "extinct" at different time bins, as fitted by RF.

Table 1B. Results of AIC analysis for three competing models performing. Table reports AIC, conditional R^2, and Accuracy (with associated standard deviation) values for three different competing models. The models are estimated for each landscape metric separately.

Metric	Relationship	AIC	Conditional R^2	Accuracy
Aggregation Index	linear	-602507.1	0.704	0.7655 (0.005)
	Linear+quadratic	-604289.4	0.707	0.7671(0.003)
	Linear+quadratic+cubic	-605018.9	0.707	0.7678 (0.003)
Mean Patch Area	linear	298319.4	0.735	0.8201 (0.002)
	Linear+quadratic	297729	0.736	0.8205 (0.001)
	Linear+quadratic+cubic	297204	0.736	0.8209 (0.002)

Mean euclidean nearest-neighbor distance	linear	-242481.6	0.431	0.6290 (0.001)
	Linear+quadratic	-242566.4	0.432	0.6291(0.007)
	Linear+quadratic+cubic	-242663.3	0.432	0.6293 (0.004)
Number of Patches	linear	163514.4	0.672	0.7955 (0.001)
	Linear+quadratic	162464.8	0.673	0.7963 (0.003)
	Linear+quadratic+cubic	162296.9	0.673	0.7964 (0.003)
Total Area	linear	263423.8	0.823	0.8941 (0.003)
	Linear+quadratic	260748.9	0.824	0.8951 (0.003)
	Linear+quadratic+cubic	259917.7	0.825	0.8954 (0.001)

Table 1B. Summary of statistics for the optimal linear mixed models as indicated by the Akaike Information Criterion. For each model, slope ("Estimate"), standard error ("St.error") and p.value referred to both extinct and extant group are reported

Metric	Status	Estimate	St.error	p.value
Aggregation Index	intercept	4.260	0.045	<0.001
	poly(time 3)1:statusextant	1.385	0.110	<0.001
	poly(time 3)2:statusextant	-3.176	0.104	<0.001
	poly(time 3)3:statusextant	1.207	0.103	<0.001
	poly(time 3)1:statusextint	4.549	0.189	<0.001
	poly(time 3)2:statusextint	-5.596	0.193	<0.001
	poly(time 3)3:statusextint	4.705	0.192	<0.001
Mean Patch Area	intercept	15.380	0.256	<0.001
	poly(time 3)1:statusextant	3.165	0.496	<0.001
	poly(time 3)2:statusextant	-8.468	0.467	<0.001
	poly(time 3)3:statusextant	1.721	0.461	<0.001
	poly(time 3)1:statusextint	12.387	0.849	<0.001
	poly(time 3)2:statusextint	-13.784	0.870	<0.001
	poly(time 3)3:statusextint	19.575	0.864	<0.001
Mean Patch Distance	intercept	12.112	0.051	<0.001
	poly(time 3)1:statusextant	1.399	0.202	<0.001
	poly(time 3)2:statusextant	-0.963	0.190	<0.001
	poly(time 3)3:statusextant	1.892	0.188	<0.001
	poly(time 3)1:statusextint	-0.637	0.345	0.065
	poly(time 3)2:statusextint	2.483	0.354	<0.001
	poly(time 3)3:statusextint	-0.361	0.351	0.304
Number of Patches	intercept	4.506	0.112	<0.001
	poly(time 3)1:statusextant	0.604	0.396	0.127
	poly(time 3)2:statusextant	-5.004	0.373	<0.001
	poly(time 3)3:statusextant	-4.482	0.368	<0.001
	poly(time 3)1:statusextint	12.792	0.678	<0.001
	poly(time 3)2:statusextint	-20.516	0.695	<0.001

	poly(time 3)3:statusextint	3.312	0.690	<0.001
Total Patch Area	intercept	19.885	0.332	<0.001
	poly(time 3)1:statusextant	3.771	0.466	<0.001
	poly(time 3)2:statusextant	-13.473	0.439	<0.001
	poly(time 3)3:statusextant	-2.762	0.434	<0.001
	poly(time 3)1:statusextint	25.181	0.798	<0.001
	poly(time 3)2:statusextint	-34.302	0.818	<0.001
	poly(time 3)3:statusextint	22.886	0.812	<0.001

The results of our approach indicate that extinct mammals went through considerable deterioration of habitat geographic structure during the last glacial period, and fared worse than extant species starting at some 50 ka (Figure 12). This suggests climatic change had a strong effect on species survival, forcing extinct species into progressively smaller and more isolated patches of suitable habitats, conceivably contributing to their final demise this way. To the late Pleistocene Eurasian large mammals, the best condition was to occur in several well-connected habitat patches, which understandably provide better chance to survive to (local) habitat deterioration and could indicate more plastic ecological tolerance.

In term of landscape structure, starting from 50 ka, extinct megafauna started to acquire a different geographic habitat structure with less and more isolated patches compared to extant species. Although derived from mathematical modeling, this date coincides nicely well with known species extinction dates. The best radiometric estimates for the extinction date of *Homo neanderthalensis* (Higham et al. 2014), the camel *Camelus knoblochi*, the giant deer *Sinomegaceros yabei*, the narrow-nosed rhino *Stephanorhinus hemitoechus*, the giant rhino *Elasmotherium sibiricum* (Kosintsev et al. 2019) the antelope *Spiroceros kiakhtensis* and the Asian straight-tusked elephant *Palaeoloxodon neumanni* occurred all within a narrow 45 to 37 ka interval (Stuart & Lister 2012). Moreover, studies on the mitochondrial DNA and population demographics suggested the cave bear *Ursus spelaeus* had a dramatic population decline starting at 50 ka (Stiller et al. 2010, Mondanaro et al. 2019). The same rapid population decline in the same time interval in Eurasia pertain to cave lion *Panthera leo spelaea* (Stuart & Lister 2011) and spotted hyena *Crocuta crocuta* (Stuart & Lister 2014). It is important to notice that all of these extinction predate and are geographically separated from the arrival of *Homo sapiens* in Eurasia (Hublin et al. 2020) indicating that it was climate

change, rather than human activity, the reason for increased patchiness in habitat structure and hence the main reason for extinction in these species. Our modelling results indicate that mean patch area and total range size for the extinct species only decrease+ much later, pointing to climate-driven habitat fragmentation as the main process for extinction. Intriguingly, most extinct megafauna species and those which survived inhabited Mediterranean area and the far East before extinction, abandoning the Northern latitudes first and separating in a number of geographical demes (Stuart & Lister 2014; Stuart & Lister 2011; Mondanaro et al. 2019; Fabre et al. 2009). In fact, the presence of glacial cryptic northern refugia could have increased habitat patchiness for the Eurasian megafauna as a whole (Bhagwat & Willis 2008; Hewitt 2000) forcing species into small separated areas. The consequences on the species survival were dramatic, although for some time the total diversity of Eurasia held a rich mixture of warm-loving and cold-loving taxa.

Our results corroborated the finding of the Saura's paper and Melchionna et al. 2018. At regional scale, habitat fragmentation implies a negative effect on species richness and these habitat configuration effects are distinct from those of habitat amount in the local landscape. Consequently, we argued conservation strategies cannot focus only on the local amount of habitat, but they should consider the entire regional habitat configuration of the focal species.

Conclusions

We demonstrated that climatic changes played a key role for the extinction of at least three human species: *H. erectus*, *H. heidelbergensis*, and *H. neanderthalensis*. Starting from Middle Pleistocene, cultural and social innovations related to advanced cognitive skills gave enormous advantages to human species to inhabit almost Old Word. Nevertheless, the more advanced material culture and possibly superior cognitive abilities, combined with a large reservoir of African individuals made *H. sapiens* the only modern human species able to survive today. As proof of this, we found *Homo sapiens* had greater ecological plasticity over Neanderthals, which probably allowed this species to better counter the colder climatic condition at 44 and then at 40 ka, a date that almost coincides with estimated Neanderthal's extinction and the onset of Heinrich Events. Moreover, we offered evidences in favor of a social interactions between *H. sapiens* and Neanderthals. This

led to a consequent genomic introgression of Neanderthal genome into present human population. These evidences questioned the onset of competitive exclusion phenomenon between these two human species. We demonstrated climatic changes were fully involved in megafauna extinction on Eurasiatic continent. Our multiple investigations shown that the climatic-driven habitat fragmentation negatively affected the survival of extinct species. Our results suggested that both size and shape of habitat patches should be considered in biodiversity conservation planning.

References

1. Aiello-Lammens, M. E., & Akçakaya, H. R. (2017). Using global sensitivity analysis of demographic models for ecological impact assessment. Conservation Biology, 31(1), 116-125.
2. Akaikei, H. (1973). Information theory and an extension of maximum likelihood principle. In Proc. 2nd Int. Symp. on Information Theory (pp. 267-281).
3. Akcakaya, H. R. & Root,W. T. 2013: RAMAS GIS: linking spatial data with population viability analysis (version 6.0). Applied Biomathematics, Setauket
4. Alley, R. B. (2000). The Younger Dryas cold interval as viewed from central Greenland. Quaternary science reviews, 19(1-5), 213-226.
5. Amanzougaghene, N., Fenollar, F., Raoult, D., & Mediannikov, O. (2019). Where are we with human lice? A review of the current state of knowledge. Frontiers in Cellular and Infection Microbiology, 9.
6. Anderson, B. J., Akcakaya, H. R., Araujo, M. B., Fordham, D. A., Martinez-Meyer, E., Thuiller, W. & Brook, B. W. 2009: Dynamics of range margins for metapopulations under climate change. Proceedings of the Royal Society B: Biological Sciences 276, 1415–142
7. Antón, S. C., & Josh Snodgrass, J. (2012). Origins and evolution of genus Homo: new perspectives. Current Anthropology, 53(S6), S479-S496.
8. Antón, S. C., Potts, R., & Aiello, L. C. (2014). Evolution of early Homo: An integrated biological perspective. Science, 345(6192).
9. Baca, M., Mackiewicz, P., Stankovic, A., Popovic, D., Stefaniak, K., Czarnogorska, K., Nadachowski, A., Ga zsiorowski, M., Hercman, H. & Weglenski, P. 2014: Ancient DNA and dating of cave bear remains from Niedzwiedzia Cave suggest early appearance of Ursus ingressus in Sudetes. Quaternary International 339, 217–223
10. Baca, M., Popovic, D., Stefaniak, K., Marciszak, A., Urbanowski, M., Nadachowski, A. & Mackiewicz, P. 2016: Retreat and extinction of the Late Pleistocene cave bear (Ursus spelaeus sensulato). The Science of Nature 103, 11–12.

11. Banks, W. E., d'Errico, F., Peterson, A. T., Kageyama, M., Sima, A., & Sánchez-Goñi, M. F. (2008). Neanderthal extinction by competitive exclusion. PLoS One, 3(12), e3972.
12. Bar-Yosef, O. (2002). The upper paleolithic revolution. Annual Review of Anthropology, 31(1), 363-393.
13. Bar-Yosef, O. (2007). The archaeological framework of the Upper Paleolithic revolution. Diogenes, 54(2), 3-18.
14. Benazzi, S., Douka, K., Fornai, C., Bauer, C. C., Kullmer, O., Svoboda, J., ... & Condemi, S. (2011). Early dispersal of modern humans in Europe and implications for Neanderthal behaviour. Nature, 479(7374), 525-528.
15. Benito, B. M., Svenning, J. C., Kellberg-Nielsen, T., Riede, F., Gil-Romera, G., Mailund, T., ... & Sandel, B. S. (2017). The ecological niche and distribution of Neanderthals during the Last Interglacial. Journal of Biogeography, 44(1), 51-61.
16. Bhagwat, S. A., & Willis, K. J. (2008). Species persistence in northerly glacial refugia of Europe: a matter of chance or biogeographical traits?. Journal of Biogeography, 35(3), 464-482.
17. Bhagwat, S. A., & Willis, K. J. (2008). Species persistence in northerly glacial refugia of Europe: a matter of chance or biogeographical traits?. Journal of Biogeography, 35(3), 464-482.
18. Blomqvist, D., Pauliny, A., Larsson, M., & Flodin, L. Å. (2010). Trapped in the extinction vortex? Strong genetic effects in a declining vertebrate population. BMC Evolutionary Biology, 10(1), 33.
19. Bocquet-Appel, J. P., & Degioanni, A. (2013). Neanderthal demographic estimates. Current Anthropology, 54(S8), S202-S213.
20. Bocquet-Appel, J.-P. & Demars, P.-Y. 2000: Population kinetics in the upper Palaeolithic in Western Europe. Journal of Archaeological Science 27, 551–570
21. Botta, F., Dahl-Jensen, D., Rahbek, C., Svensson, A., & Nogués-Bravo, D. (2019). Abrupt change in climate and biotic systems. Current Biology, 29(19), R1045-R1054.
22. Box, G. E., & Cox, D. R. (1964). An analysis of transformations. Journal of the Royal Statistical Society: Series B (Methodological), 26(2), 211-243.

23. Braunisch, V., Bollmann, K., Graf, R. F., & Hirzel, A. H. (2008). Living on the edge—modelling habitat suitability for species at the edge of their fundamental niche. Ecological modelling, 214(2-4), 153-167.
24. Broennimann, O., Fitzpatrick, M. C., Pearman, P. B., Petitpierre, B., Pellissier, L., Yoccoz, N. G., ... & Graham, C. H. (2012). Measuring ecological niche overlap from occurrence and spatial environmental data. Global ecology and biogeography, 21(4), 481-497.
25. Burney, D. A., & Flannery, T. F. (2005). Fifty millennia of catastrophic extinctions after human contact. Trends in Ecology & Evolution, 20(7), 395-401.
26. Calenge, C. (2006). The package "adehabitat" for the R software: a tool for the analysis of space and habitat use by animals. Ecological modelling, 197(3-4), 516-519.
27. Cârciumaru, M., Ion, R. M., Niţu, E. C., & Ştefănescu, R. (2012). New evidence of adhesive as hafting material on Middle and Upper Palaeolithic artefacts from Gura Cheii-Râşnov Cave (Romania). Journal of Archaeological Science, 39(7), 1942-1950.
28. Carotenuto, F., Di Febbraro, M., Melchionna, M., Castiglione, S., Saggese, F., Serio, C., ... & Raia, P. (2016). The influence of climate on species distribution over time and space during the late Quaternary. Quaternary Science Reviews, 149, 188-199.
29. Carotenuto, F., Di Febbraro, M., Melchionna, M., Mondanaro, A., Castiglione, S., Serio, C., ... & Raia, P. (2018). The well-behaved killer: Late Pleistocene humans in Eurasia were significantly associated with living megafauna only. Palaeogeography, Palaeoclimatology, Palaeoecology, 500, 24-32.
30. Castiglione, S., Serio, C., Mondanaro, A., Di Febbraro, M., Profico, A., Girardi, G., & Raia, P. (2019). Simultaneous detection of macroevolutionary patterns in phenotypic means and rate of change with and within phylogenetic trees including extinct species. PloS one, 14(1), e0210101.
31. Castiglione, S., Tesone, G., Piccolo, M., Melchionna, M., Mondanaro, A., Serio, C., ... & Raia, P. (2018). A new method for testing evolutionary rate variation and shifts in phenotypic evolution. Methods in Ecology and Evolution, 9(4), 974-983.

32. Cornejo-Denman, L., Romo-Leon, J. R., Hartfield, K., van Leeuwen, W. J., Ponce-Campos, G. E., & Castellanos-Villegas, A. (2020). Landscape dynamics in an iconic watershed of Northwestern Mexico: Vegetation condition insights using landsat and planetscope data. Remote Sensing, 12(16), 2519.
33. D'Amen, M., Dubuis, A., Fernandes, R. F., Pottier, J., Pellissier, L., & Guisan, A. (2015). Using species richness and functional traits predictions to constrain assemblage predictions from stacked species distribution models. *Journal of Biogeography*, *42*(7), 1255–1266. doi: 10.1111/jbi.12485
34. Dannemann, M. (2020). The population-specific impact of Neandertal introgression on human disease. Genome Biology and Evolution.
35. Dannemann, M., & Kelso, J. (2017). The contribution of Neanderthals to phenotypic variation in modern humans. The American journal of human genetics, 101(4), 578-589.
36. Di Febbraro, M., Carotenuto, F., Castiglione, S., Russo, D., Loy, A., Maiorano, L., & Raia, P. (2017). Does the jack of all trades fare best? Survival and niche width in Late Pleistocene megafauna. Journal of Biogeography, 44(12), 2828-2838.
37. Di Febbraro, M., Roscioni, F., Frate, L., Carranza, M. L., De Lisio, L., De Rosa, D., ... & Loy, A. (2015). Long-term effects of traditional and conservation-oriented forest management on the distribution of vertebrates in Mediterranean forests: a hierarchical hybrid modelling approach. Diversity and Distributions, 21(10), 1141-1154.
38. Diamond, J. (1989). The great leap forward. Discover, 10(5), 50-60.
39. Dufresne, E.R., Saltré, F., Cooke, B.D., Mellin, C., Mutze, G., Cox, T., et al. (2019). Modeling the distribution of a wide-ranging invasive species using the sampling efforts of expert and citizen scientists. Ecol Evol, 9, 11053–11063.
40. Ellison, P. T., & Valeggia, C. R. (2005). 13 Human birth seasonality. Seasonality in primates: Studies of living and extinct human and non-human primates, 44, 379.
41. Fabre, V., Condemi, S., & Degioanni, A. (2009). Genetic evidence of geographical groups among Neanderthals. PloS one, 4(4), e5151.

42. Fahrig, L. (2013). Rethinking patch size and isolation effects: the habitat amount hypothesis. Journal of Biogeography, 40(9), 1649-1663.
43. Fahrig, L. (2020). Why do several small patches hold more species than few large patches?. Global Ecology and Biogeography, 29(4), 615-628.
44. Fahrig, L. What the habitat amount hypothesis does and does not predict: A reply to Saura. Journal of Biogeography.
45. Faith, J. T., & Surovell, T. A. (2009). Synchronous extinction of North America's Pleistocene mammals. Proceedings of the National Academy of Sciences, 106(49), 20641-20645.
46. Firestone, R. B., West, A., Kennett, J. P., Becker, L., Bunch, T. E., Revay, Z. S., ... & Dickenson, O. J. (2007). Evidence for an extraterrestrial impact 12,900 years ago that contributed to the megafaunal extinctions and the Younger Dryas cooling. Proceedings of the National Academy of Sciences, 104(41), 16016-16021.
47. Fourcade, Y., Besnard, A. G., & Secondi, J. (2018). Paintings predict the distribution of species, or the challenge of selecting environmental predictors and evaluation statistics. Global Ecology and Biogeography, 27(2), 245-256.
48. Fourcade, Y., Besnard, A.G. & Secondi, J. (2018). Paintings predict the distribution of species, or the challenge of selecting environmental predictors and evaluation statistics. Global Ecology and Biogeography, 27, 245–256.
49. Freeman, E. A., & Moisen, G. (2008). PresenceAbsence: An R package for presence absence analysis. Journal of Statistical Software. 23 (11): 31 p.
50. Fritz, H., Duncan, P., Gordon, I. J., & Illius, A. W. (2002). Megaherbivores influence trophic guilds structure in African ungulate communities. Oecologia, 131(4), 620-625.
51. Fu, Q., Hajdinjak, M., Moldovan, O. T., Constantin, S., Mallick, S., Skoglund, P., ... & Viola, B. (2015). An early modern human from Romania with a recent Neanderthal ancestor. Nature, 524(7564), 216-219.
52. Fuentes, A., Wyczalkowski, M. A., & MacKinnon, K. C. (2010). Niche construction through cooperation: a nonlinear dynamics contribution to modeling facets of the evolutionary history in the genus Homo. Current Anthropology, 51(3), 435-444.

53. Gajewski, K., Muñoz, S., Peros, M., Viau, A., Morlan, R., & Betts, M. (2011). The Canadian archaeological radiocarbon database (CARD): archaeological 14 C dates in North America and their paleoenvironmental context. Radiocarbon, 53(2), 371-394.

54. Gaudzinski, S., Turner, E., Anzidei, A. P., Àlvarez-Fernández, E., Arroyo-Cabrales, J., Cinq-Mars, J., ... & Scheer, A. (2005). The use of Proboscidean remains in every-day Palaeolithic life. Quaternary International, 126, 179-194.

55. Gavish, Y., Ziv, Y., & Rosenzweig, M. L. (2012). Decoupling fragmentation from habitat loss for spiders in patchy agricultural landscapes. Conservation Biology, 26(1), 150-159.

56. Gervasi, V.& Ciucci, P. 2018: Demographic projections of the Apennine brown bear population Ursus arctos marsicanus (Mammalia: Ursidae) under alternative management scenarios. The European Zoological Journal 85, 243–253.

57. Gervasi, V., Nilsen, E. B., Sand, H., Panzacchi, M., Rauset, G. R., Pedersen, H. C., Kindberg, J., Wabakken, P., Zimmermann, B., Odden, J., Liberg, O., Swenson, J. E. & Linnell, J. D. C. 2011: Predicting the potential demographic impact of predators on their prey: a comparative analysis of two carnivore-ungulate systems in Scandinavia. Journal of Animal Ecology 81, 443–454.

58. Gilligan, I. (2007). Neanderthal extinction and modern human behaviour: the role of climate change and clothing. World Archaeology, 39(4), 499-514.

59. Gilpin, W., Feldman, M. W., & Aoki, K. (2016). An ecocultural model predicts Neanderthal extinction through competition with modern humans. Proceedings of the National Academy of Sciences, 113(8), 2134-2139.

60. Gislason, P. O., Benediktsson, J. A., & Sveinsson, J. R. (2006). Random forests for land cover classification. Pattern Recognition Letters, 27(4), 294-300.

61. Gislason, P. O., Benediktsson, J. A., & Sveinsson, J. R. (2006). Random forests for land cover classification. Pattern recognition letters, 27(4), 294-300.

62. Gowlett, J. A. (2016). The discovery of fire by humans: a long and convoluted process. Philosophical Transactions of the Royal Society B: Biological Sciences, 371(1696), 20150164.

63. Green, R. E., Krause, J., Briggs, A. W., Maricic, T., Stenzel, U., Kircher, M., ... & Hansen, N. F. (2010). A draft sequence of the Neandertal genome. science, 328(5979), 710-722.
64. Greenbaum, G., Friesem, D. E., Hovers, E., Feldman, M. W., & Kolodny, O. (2019). Was inter-population connectivity of Neanderthals and modern humans the driver of the Upper Paleolithic transition rather than its product? Quaternary Science Reviews, 217, 316-329.
65. Guthrie, R. D. (2003). Rapid body size decline in Alaskan Pleistocene horses before extinction. Nature, 426(6963), 169-171.
66. Halligan, J. J., Waters, M. R., Perrotti, A., Owens, I. J., Feinberg, J. M., Bourne, M. D., ... & Stafford, T. W. (2016). Pre-Clovis occupation 14,550 years ago at the Page-Ladson site, Florida, and the peopling of the Americas. Science advances, 2(5), e1600375.
67. Hanski, I. (2015). Habitat fragmentation and species richness. Journal of Biogeography, 42, 989–994.
68. Hardy, B. L., Moncel, M. H., Kerfant, C., Lebon, M., Bellot-Gurlet, L., & Mélard, N. (2020). Direct evidence of Neanderthal fibre technology and its cognitive and behavioral implications. Scientific reports, 10(1), 1-9.
69. He, H. S., DeZonia, B. E., & Mladenoff, D. J. (2000). An aggregation index (AI) to quantify spatial patterns of landscapes. Landscape Ecology, 15(7), 591–601.
70. Hesselbarth, M. H., Sciaini, M., With, K. A., Wiegand, K., & Nowosad, J. (2019). landscapemetrics: an open-source R tool to calculate landscape metrics. Ecography, 42(10), 1648-1657.
71. Hewitt, G. (2000). The genetic legacy of the Quaternary ice ages. Nature, 405(6789), 907-913.
72. Hewitt, G. (2000). The genetic legacy of the Quaternary ice ages. Nature, 405(6789), 907-913.
73. Higham, T., Douka, K., Wood, R., Ramsey, C. B., Brock, F., Basell, L., ... & Bergman, C. (2014). The timing and spatiotemporal patterning of Neanderthal disappearance. Nature, 512(7514), 306-309.
74. Hirzel, A. H., Le Lay, G., Helfer, V., Randin, C., & Guisan, A. (2006). Evaluating the ability of habitat suitability models to predict species presences. Ecological modelling, 199(2), 142-152.
75. Hiscock, P. (2014). Learning in lithic landscapes: a reconsideration of the hominid “toolmaking” niche. Biological Theory, 9(1), 27-41.

76. Ho, S. Y. W. & Shapiro, B. 2011: Skyline-plot methods for estimating demographic history from nucleotide sequences. Molecular Ecology Resources 11, 423–434.

77. Holdaway, R. N., Allentoft, M. E., Jacomb, C., Oskam, C. L., Beavan, N. R., & Bunce, M. (2014). An extremely low-density human population exterminated New Zealand moa. Nature Communications, 5(1), 1-8.

78. Holden, P. B., Edwards, N R., Rangel, T. F., Pereira, E. B., Tran, G. T., & Wllkinson, R. D. (2019). PALEO-PGEM v1. 0: a statistical emulator of Pliocene–Pleistocene climate. Geoscientific Model Development, 12(12), 5137-5155.

79. Hortolà, P., & Martínez-Navarro, B. (2013). The Quaternary megafaunal extinction and the fate of Neanderthals: An integrative working hypothesis. Quaternary International, 295, 69-72.

80. Hublin, J. J., Sirakov, N., Aldeias, V., Bailey, S., Bard, E., Delvigne, V., ... & Kromer, B. (2020). Initial Upper Palaeolithic Homo sapiens from Bacho Kiro Cave, Bulgaria. Nature, 1-4.

81. Jaubert, J., Verheyden, S., Genty, D., Soulier, M., Cheng, H., Blamart, D., ... & Edwards, R. L. (2016). Early Neanderthal constructions deep in Bruniquel Cave in southwestern France. Nature, 534(7605), 111-114.

82. Johnson, C. N., Bradshaw, C. J., Cooper, A., Gillespie, R., & Brook, B. W. (2013). Rapid megafaunal extinction following human arrival throughout the New World. Quaternary International, 308, 273-277.

83. Jones, K. E., Bielby, J., Cardillo,M., Fritz, S. A., O'Dell, J., Orme, C. D. L., Safi, K., Sechrest, W., Boakes, E. H., Carbone, C., Connolly, C., Cutts,M. J.,Foster, J.K.,Grenyer,R.,Habib,M., Plaster, C.A., Price, S. A., Rigby, E. A., Rist, J., Teacher, A., Bininda-Emonds, O. R. P., Gittleman, J. L., Mace, J. M. & Purvis, A. 2009: PanTHERIA: a species-level database oflife history, ecology, and geographyof extant and recently extinct mammals. Ecology 90, 2648–2648

84. Karger, D. N., Conrad, O., Böhner, J., Kawohl, T., Kreft, H., Soria-Auza, R. W., ... & Kessler, M. (2017). Climatologies at high resolution for the earth's land surface areas. Scientific data, 4(1), 1-20.

85. Kathleen Lyons, S., Smith, F. A., Wagner, P. J., White, E. P., & Brown, J. H. (2004). Was a 'hyperdisease' responsible for the late Pleistocene megafaunal extinction? Ecology Letters, 7(9), 859-868.

86. Keller, L. F., & Waller, D. M. (2002). Inbreeding effects in wild populations. Trends in ecology & evolution, 17(5), 230-241.

87. Kosintsev, P., Mitchell, K. J., Devièse, T., van der Plicht, J., Kuitems, M., Petrova, E., ... & Cooper, A. (2019). Evolution and extinction of the giant rhinoceros Elasmotherium sibiricum sheds light on late Quaternary megafaunal extinctions. Nature ecology & evolution, 3(1), 31-38.

88. Kuhn, M., Wing, J., Weston, S., Williams, A., Keefer, C., Engelhardt, A., ... & Benesty, M. (2020). Package 'caret'. The R Journal.

89. Laland, K. N., & O'brien, M. J. (2011). Cultural niche construction: An introduction. Biological Theory, 6(3), 191-202.

90. Laland, K. N., Kendal, J. R., & Brown, G. R. (2007). The niche construction perspective: Implications for evolution and human behaviour. Journal of Evolutionary Psychology, 5(1), 51-66.

91. Laland, K. N., Odling-Smee, J., & Feldman, M. W. (2001). Cultural niche construction and human evolution. Journal of evolutionary biology, 14(1), 22-33.

92. Lande, R. & Barrowclough, G. F. 1987: Effective population size, genetic variation, and their use in population management.In Soule, M. E. (ed.): Viable Populations in Conservation, 87–124. Sinauer Associates, Sunderland.

93. Lefkovitch, L. P. 1965: The study of population growth in organisms grouped by stages. Biometrics 21, 1–18.

94. Lenoir, M., & Villa, P. (2006). Hunting weapons of the Middle Stone Age and the Middle Palaeolithic: spear points from Sibudu, Rose Cottage and Bouheben. Southern African Humanities, 18(1), 89-122.

95. Lewontin, R. C. (1983). Gene, organism and environment. Evolution from molecules to men, 273, 285.

96. Liu, C., Berry, P. M., Dawson, T. P., & Pearson, R. G. (2005). Selecting thresholds of occurrence in the prediction of species distributions. Ecography, 28(3), 385-393.

97. Liu, X., Pei, F., Wen, Y., Li, X., Wang, S., Wu, C., *et al.* (2019). Global urban expansion offsets climate-driven increases in terrestrial net primary productivity. *Nature Communications*, 10, 5558–8.

98. Lorenzen, E. D., Nogués-Bravo, D., Orlando, L., Weinstock, J., Binladen, J., Marske, K. A., ... & Ho, S. Y. (2011). Species-specific responses of Late Quaternary megafauna to climate and humans. Nature, 479(7373), 359-364.

99. Loy, A., Genov, P., Galfo, M., Jacobone, M. G. & Vigna Taglianti, A. 2008: Cranial morphometrics of the Apennine brown bear (Ursus arctos marsicanus) and preliminary notes on the relationships with other southern European populations.Italian Journal of Zoology 75, 67–75

100. Mac Nally, R., & Lake, P. S. (1999). On the generation of diversity in archipelagos: A re-evaluation of the Quinn-Harrison "saturation index". Journal of Biogeography, 26, 285–295.

101. Maiorano, L., Cheddadi, R., Zimmermann, N. E., Pellissier, L., Petitpierre, B., Pottier, J., ... & Singarayer, J. S. (2013). Building the niche through time: using 13,000 years of data to predict the effects of climate change on three tree species in Europe. Global Ecology and Biogeography, 22(3), 302-317.

102. Malhi, Y., Doughty, C. E., Galetti, M., Smith, F. A., Svenning, J. C., & Terborgh, J. W. (2016). Megafauna and ecosystem function from the Pleistocene to the Anthropocene. Proceedings of the National Academy of Sciences, 113(4), 838-846.

103. Mann, D. H., Groves, P., Gaglioti, B. V., & Shapiro, B. A. (2019). Climate-driven ecological stability as a globally shared cause of Late Quaternary megafaunal extinctions: the Plaids and Stripes Hypothesis. Biological Reviews, 94(1), 328-352.

104. Marmion, M., Parviainen, M., Luoto, M., Heikkinen, R. K., & Thuiller, W. (2009). Evaluation of consensus methods in predictive species distribution modelling. Diversity and distributions, 15(1), 59-69.

105. Marshall, S. J. & Koutnik, M. R. 2006: Ice sheet action versus reaction: distinguishing between Heinrich events and Dansgaard-Oeschger cycles in the North Atlantic. Paleoceanography 21, PA2021, https:// doi.org/10.1029/2005pa001247

106. Martin, P. S. (1973). The Discovery of America: The first Americans may have swept the Western Hemisphere and decimated its fauna within 1000 years. Science, 179(4077), 969-974.

107. McGarigal, K., Cushman, S. A., & Ene, E. (2012). FRAGSTATS v4: spatial pattern analysis program for categorical and continuous maps. Computer software program produced by the authors at the University of Massachusetts, Amherst.

108. Melchionna, M., Di Febbraro, M., Carotenuto, F., Rook, L., Mondanaro, A., Castiglione, S., ... & Raia, P. (2018). Fragmentation of Neanderthals' pre-extinction distribution by climate change. Palaeogeography, palaeoclimatology, palaeoecology, 496, 146-154.

109. Melchionna, M., Mondanaro, A., Serio, C., Castiglione, S., Di Febbraro, M., Rook, L., ... & Raia, P. (2020). Macroevolutionary trends of brain mass in Primates. Biological Journal of the Linnean Society, 129(1), 14-25.

110. Merow, C., Smith, M. J., & Silander, J. A. (2013). A practical guide to MaxEnt for modeling species' distributions: what it does, and why inputs and settings matter. Ecography, 36(10), 1058–1069. doi: 10.1111/j.1600-0587.2013.07872.x

111. Mondanaro, A., Castiglione, S., Melchionna, M., Di Febbraro, M., Vitagliano, G., Serio, C., ... & Raia, P. (2017). Living with the elephant in the room: top-down control in Eurasian large mammal diversity over the last 22 million years. Palaeogeography, palaeoclimatology, palaeoecology, 485, 956-962.

112. Mondanaro, A., Di Febbraro, M., Melchionna, M., Carotenuto, F., Castiglione, S., Serio, C., ... & Raia, P. (2019). Additive effects of climate change and human hunting explain population decline and extinction in cave bears. Boreas, 48(3), 605-615.

113. Mondanaro, A., Melchionna, M., Di Febbraro, M., Castiglione, S., Holden, P. B., Edwards, N. R., ... & Raia, P. (2020). A major change in rate of climate niche envelope evolution during hominid history. Iscience, 23(11), 101693.

114. Munzel, S. C., Stiller, M., Hofreiter, M., Mittnik, A., Conard, N. J. & € Bocherens, H. 2011: Pleistocene bears in the Swabian Jura (Germany): genetic replacement, ecological displacement, extinctions and survival. Quaternary International 245, 225–237

115. Muscarella, R., Galante, P.J., Guardia, M.S., Boria, R.A., Kass, J.M., Uriarte, M., et al. (2014). ENMeval: An R package for conducting spatially independent evaluations and estimating optimal model complexity for Maxent ecological niche models. Methods in Ecology and Evolution, 5, 1198–1205.

116. Nakagawa, S., & Schielzeth, H. (2013). A general and simple method for obtaining R2 from generalized linear mixed-effects models. Methods in ecology and evolution, 4(2), 133-142.

117. Organ, C., Nunn, C. L., Machanda, Z., & Wrangham, R. W. (2011). Phylogenetic rate shifts in feeding time during the evolution of Homo. Proceedings of the National Academy of Sciences, 108(35), 14555-14559.

118. Parfitt, S. A., Ashton, N. M., Lewis, S. G., Abel, R. L., Coope, G. R., Field, M. H., ... & Karloukovski, V. (2010). Early Pleistocene human occupation at the edge of the boreal zone in northwest Europe. Nature, 466(7303), 229-233.

119. Pellettier, J. D. (2000). Model assessments of the optimal design of nature reserves for maximizing species longevity. Journal of Theoretical Biology, 202(1), 25-32.

120. Perry, G. L. W., Wheeler, A. B., Wood, J. R. & Wilmshurst, J. M. (2014). A high-precision chronology for the rapid extinction of New Zealand moa (Aves, Dinornithiformes). Quaternary Science Reviews 105, 126–135

121. Phillips, S. J., & Dudík, M. (2008). Modeling of species distributions with Maxent: new extensions and a comprehensive evaluation. Ecography, 31(2), 161-175.

122. Phillips, S. J., Anderson, R. P., & Schapire, R. E. (2006). Maximum entropy modeling of species geographic distributions. Ecological modelling, 190(3-4), 231-259.

123. Price, G., Louys, J., Faith, J., Lorenzen, E. & Westaway, M. (2018). Big data little help in megafauna mysteries. Nature 558, 23

124. Profico, A., Di Vincenzo, F., Gagliardi, L., Piperno, M., & Manzi, G. (2016). Filling the gap. Human cranial remains from Gombore II (Melka Kunture, Ethiopia; ca. 850 ka) and the origin of Homo heidelbergensis. Journal of Anthropological Sciences, 94, 1-24.

125. Raia, P., Mondanaro, A., Melchionna, M., Di Febbraro, M., Diniz-Filho, J. A., Rangel, T. F., ... & Rook, L. (2020). Past extinctions of Homo species coincided with increased vulnerability to climatic change. One Earth, 3(4), 480-490.

126. Raia, P., Boggioni, M., Carotenuto, F., Castiglione, S., Di Febbraro, M., Di Vincenzo, F., ... & Serio, C. (2018). Unexpectedly rapid evolution of mandibular shape in hominins. Scientific reports, 8(1), 1-8.

127. Raia, P., Carotenuto, F., Meloro, C., Piras, P., Barbera, C., & Kotsakis, T. (2009). More than three million years of community evolution. The temporal and geographical resolution of the Plio-Pleistocene Western Eurasia mammal faunas. Palaeogeography, Palaeoclimatology, Palaeoecology, 276(1-4), 15-23.

128. Rasmussen, S. O., Andersen, K. K., Svensson, A. M., Steffensen, J. P., Vinther, B. M., Clausen, H. B., ... & Bigler, M. (2006). A new Greenland ice core chronology for the last glacial termination. Journal of Geophysical Research: Atmospheres, 111(D6).

129. Reimer, P. J., Austin, W. E., Bard, E., Bayliss, A., Blackwell, P. G., Ramsey, C. B., ... & Grootes, P. M. (2020). The IntCal20 Northern Hemisphere radiocarbon age calibration curve (0–55 cal kBP). Radiocarbon, 62(4), 725-757.

130. Rightmire, G. P., & Lordkipanidze, D. (2009). Comparisons of early Pleistocene skulls from East Africa and the Georgian Caucasus: evidence bearing on the origin and systematics of genus Homo. In The First Humans–Origin and Early Evolution of the Genus Homo (pp. 39-48). Springer, Dordrecht.

131. Rinnan, D. S., & Lawler, J. (2019). Climate-niche factor analysis: a spatial approach to quantifying species vulnerability to climate change. Ecography, 42(9), 1494-1503.

132. Ripple, W. J., & Van Valkenburgh, B. (2010). Linking top-down forces to the Pleistocene megafaunal extinctions. BioScience, 60(7), 516-526.

133. Romandini, M., Terlato, G., Nannini, N., Tagliacozzo, A., Benazzi, S.& Peresani, M. 2018: Bears and humans, a Neanderthal tale. Reconstructing uncommon behaviors from zooarchaeological evidence in southern Europe. Journal of Archaeological Science 90, 71–91

134. Roy-Dufresne, E., Saltré, F., Cooke, B. D., Mellin, C., Mutze, G., Cox, T., & Fordham, D. A. (2019). Modeling the distribution of a wide-ranging invasive species using the sampling efforts of expert and citizen scientists. Ecology and evolution, 9(19), 11053-11063.

135. Sandom, C., Faurby, S., Sandel, B., & Svenning, J. C. (2014). Global late Quaternary megafauna extinctions linked to humans, not climate change. Proceedings of the Royal Society B: Biological Sciences, 281(1787), 20133254.

136. Sankararaman, S., Mallick, S., Dannemann, M., Prüfer, K., Kelso, J., Pääbo, S., ... & Reich, D. (2014). The genomic landscape of Neanderthal ancestry in present-day humans. Nature, 507(7492), 354-357.

137. Saura, S. (2021). The Habitat Amount Hypothesis implies negative effects of habitat fragmentation on species richness. Journal of Biogeography, 48(1), 11-22.

138. Schoener, T. W. (1970). Nonsynchronous spatial overlap of lizards in patchy habitats. Ecology, 51(3), 408-418.

139. Sepulchre, P., Ramstein, G., Kageyama, M., Vanhaeren, M., Krinner, G., Sánchez-Goñi, M. F., & d'Errico, F. (2007). H4 abrupt event and late Neanderthal presence in Iberia. Earth and Planetary Science Letters, 258(1-2), 283-292.

140. Shillito, L. M., Whelton, H. L., Blong, J. C., Jenkins, D. L., Connolly, T. J., & Bull, I. D. (2020). Pre-Clovis occupation of the Americas identified by human fecal biomarkers in coprolites from Paisley Caves, Oregon. Science advances, 6(29), eaba6404.

141. Shipman, P. (2015). How do you kill 86 mammoths? Taphonomic investigations of mammoth megasites. Quaternary International, 359, 38-46.

142. Signor, P. W., Lipps, J. H., Silver, L. T., & Schultz, P. H. (1982). Sampling bias, gradual extinction patterns, and catastrophes in the fossil record. Geological implications of impacts of large asteroids and comets on the Earth, 190, 291-296.

143. Simard, F., Ayala, D., Kamdem, G. C., Pombi, M., Etouna, J., Ose, K., ... & Costantini, C. (2009). Ecological niche partitioning between Anopheles gambiae molecular forms in Cameroon: the ecological side of speciation. BMC ecology, 9(1), 17.

144. Singarayer, J. S., & Valdes, P. J. (2010). High-latitude climate sensitivity to ice-sheet forcing over the last 120 kyr. Quaternary Science Reviews, 29(1-2), 43-55.

145. Sørensen, B. (2011). Demography and the extinction of European Neanderthals. Journal of Anthropological Archaeology, 30(1), 17-29.

146. Sørensen, B. (2011). Demography and the extinction of European Neanderthals. Journal of Anthropological Archaeology, 30(1), 17-29.

147. Soule, M. E., & Simberloff, D. (1986). What do genetics and ecology tell us about the design of nature reserves?. Biological conservation, 35(1), 19-40.

148. Spikins, P., Needham, A., Wright, B., Dytham, C., Gatta, M., & Hitchens, G. (2019). Living to fight another day: The ecological and evolutionary significance of Neanderthal healthcare. Quaternary Science Reviews, 217, 98-118.

149. Stewart, J. R. (2004). Neanderthal–modern human competition? A comparison between the mammals associated with Middle and Upper Palaeolithic industries in Europe during OIS 3. International Journal of Osteoarchaeology, 14(3-4), 178-189.

150. Stiller, M., Baryshnikov, G., Bocherens, H., Grandal d'Anglade, A., Hilpert, B., Munzel, S. C., Pinhasi, R., Rabeder, G., Rosendahl, W., € Trinkaus, E., Hofreiter, M. & Knapp, M. 2010: Withering away– 25,000 years of genetic decline preceded cave bear extinction. Molecular Biology and Evolution 27, 975–978.

151. Stiller, M., Baryshnikov, G., Bocherens, H., Grandal d'Anglade, A., Hilpert, B., Münzel, S. C., ... & Hofreiter, M. (2010). Withering away—25,000 years of genetic decline preceded cave bear extinction. Molecular biology and evolution, 27(5), 975-978.

152. Stiller, M., Molak, M., Prost, S., Rabeder, G., Baryshnikov, G., Rosendahl, W., Munzel, S., Bocherens, H., Grandal-d € 'Anglade, A., Hilpertl, B., Germonpre, M., Stasyk, O., Pinhasi, R., Tintori, A., Rohland, N., Mohandesan, E., Ho, S. Y. W., Hofreiter, M. & Knapp, M. 2014: Mitochondrial DNA diversity and evolution of the Pleistocene cave bear complex. Quaternary International 339, 224–231

153. Stiner, M. C., & Kuhn, S. L. (2006). Changes in the 'connectedness' and resilience of Paleolithic societies in Mediterranean ecosystems. Human Ecology, 34(5), 693-712.

154. Stiner,M. C., Achyuthan, H., Arsebuk, G., Howell, F. C., Josephson, S. € C., Juell, K. E., Pigati, J. & Quade, J. 2016: Reconstructing cave bear paleoecology from skeletons: a cross-disciplinary study of middle Pleistocene bears from Yarimburgaz Cave, Turkey. Paleobiology 24, 74–98

155. Stuart, A. J., & Lister, A. M. (2011). Extinction chronology of the cave lion Panthera spelaea. Quaternary Science Reviews, 30(17-18), 2329-2340.

156. Stuart, A. J., & Lister, A. M. (2012). Extinction chronology of the woolly rhinoceros Coelodonta antiquitatis in the context of late Quaternary megafaunal extinctions in northern Eurasia. Quaternary Science Reviews, 51, 1-17.

157. Stuart, A. J., & Lister, A. M. (2014). New radiocarbon evidence on the extirpation of the spotted hyaena (Crocuta crocuta (Erxl.)) in northern Eurasia. Quaternary Science Reviews, 96, 108-116.

158. Surovell, T. A., Pelton, S. R., Anderson-Sprecher, R., & Myers, A. D. (2016). Test of Martin's overkill hypothesis using radiocarbon dates on extinct megafauna. Proceedings of the National Academy of Sciences, 113(4), 886-891.

159. Swets, J. A. (1988). Measuring the accuracy of diagnostic systems. Science, 240(4857), 1285-1293.

160. Syfert, M. M., Smith, M. J., & Coomes, D. A. (2013). The effects of sampling bias and model complexity on the predictive performance of MaxEnt species distribution models. PloS one, 8(2), e55158.

161. Terlato, G., Bocherens, H., Romandini, M., Nannini, N., Hobson, K. A. & Peresani, M. 2018: Chronological and Isotopic data support a revision for the timing of cave bear extinction in Mediterranean Europe. Historical Biology, 1–11.

162. Thuiller, W., Lafourcade, B., Engler, R., & Araújo, M. B. (2009). BIOMOD–a platform for ensemble forecasting of species distributions. Ecography, 32(3), 369-373.

163. Tjørve, E. (2010). How to resolve the SLOSS debate: lessons from species-diversity models. Journal of Theoretical Biology, 264(2), 604-612.

164. Torres, T., Ortiz, J. E., Cobo, R., de Hoz, P., Garcıa-Redondo, A. & Grun, R. 2007: Hominid exploitation of the environment and cave € bear populations. The case of Ursus spelaeus Rosenmuller-Heinroth € in Amutxate cave (Aralar, Navarra-Spain). Journal of Human Evolution 52, 1–15.

165. Turk, M., Turk, I., Dimkaroski, L., Blackwell, B. A., Horusitzky, F. Z., Otte, M., ... & Korat, L. (2018). The Mousterian musical instrument from the Divje babe I cave (Slovenia): Arguments on the material evidence for Neanderthal musical behaviour. L'anthropologie, 122(4), 679-706.

166. Ulijaszek, S. J., & Strickland, S. S. (Eds.). (2009). Seasonality and human ecology (Vol. 35). Cambridge University Press.

167. Van Meerbeeck, C. J., Renssen, H., & Roche, D. M. (2009). How did Marine Isotope Stage 3 and Last Glacial Maximum climates differ?–perspectives from equilibrium simulations. Climate of the Past, 5(1), 33-51.

168. Van Peer, P. (2004). Did Middle Stone Age moderns of sub-Saharan African descent trigger an Upper Paleolithic revolution in the lower Nile Valley?. Anthropologie (1962-), 42(3), 215-226.

169. Villmoare, B., Kimbel, W. H., Seyoum, C., Campisano, C. J., DiMaggio, E. N., Rowan, J., ... & Reed, K. E. (2015). Early Homo at 2.8 Ma from Ledi-Geraru, Afar, Ethiopia. Science, 347(6228), 1352-1355.

170. Wang, X., Blanchet, F. G., & Koper, N. (2014). Measuring habitat fragmentation: an evaluation of landscape pattern metrics. Methods in Ecology and Evolution, 5(7), 634-646.

171. Waters, M. R., & Stafford, T. W. (2007). Redefining the age of Clovis: implications for the peopling of the Americas. Science, 315(5815), 1122-1126.

172. Waters, M. R., Keene, J. L., Forman, S. L., Prewitt, E. R., Carlson, D. L., & Wiederhold, J. E. (2018). Pre-Clovis projectile points at the Debra L. Friedkin site, Texas—Implications for the Late Pleistocene peopling of the Americas. Science Advances, 4(10), eaat4505.

173. Waters, M. R., Stafford, T. W., McDonald, H. G., Gustafson, C., Rasmussen, M., Cappellini, E., ... & Willerslev, E. (2011). Pre-Clovis mastodon hunting 13,800 years ago at the Manis site, Washington. Science, 334(6054), 351-353.

174. Wollstonecroft, M. M. (2011). Investigating the role of food processing in human evolution: a niche construction approach. Archaeological and Anthropological Sciences, 3(1), 141-150.

175. Wroe, S., & Field, J. (2006). A review of the evidence for a human role in the extinction of Australian megafauna and an alternative interpretation. Quaternary Science Reviews, 25(21-22), 2692-2703.

176. Wroe, S., Field, J. H., Archer, M., Grayson, D. K., Price, G. J., Louys, J., ... & Mooney, S. D. (2013). Climate change frames debate over the extinction of megafauna in Sahul (Pleistocene Australia-New Guinea). Proceedings of the National Academy of Sciences, 110(22), 8777-8781.

177. Zatelli, P., Gobbi, S., Tattoni, C., Cantiani, M. G., La Porta, N., Rocchini, D., ... & Ciolli, M. (2019). Relevance of the Cell Neighborhood Size in Landscape Metrics Evaluation and Free or Open Source Software Implementations. ISPRS International Journal of Geo-Information, 8(12), 586.

178. Zuur, A. F., Ieno, E. N., & Elphick, C. S. (2010). A protocol for data exploration to avoid common statistical problems. Methods in ecology and evolution, 1(1), 3-14.